TECHNICAL SPECIFICATION

ISO/TS 14521

First edition
2020-04

Gears — Calculation of load capacity of worm gears

Engrenages — Calcul de la capacité de charge des engrenages à vis

Reference number
ISO/TS 14521:2020(E)

ISO copyright office
CP 401 • Ch. de Blandonnet 8
CH-1214 Vernier, Geneva
Phone: +41 22 749 01 11
Fax: +41 22 749 09 47
Email: copyright@iso.org
Website: www.iso.org

Published in Switzerland

Contents

Page

Foreword

ISO (the International Organization for Standardization) is a worldwide federation of national standards bodies (ISO member bodies). The work of preparing International Standards is normally carried out through ISO technical committees. Each member body interested in a subject for which a technical committee has been established has the right to be represented on that committee. International organizations, governmental and non-governmental, in liaison with ISO, also take part in the work. ISO collaborates closely with the International Electrotechnical Commission (IEC) on all matters of electrotechnical standardization.

The procedures used to develop this document and those intended for its further maintenance are described in the ISO/IEC Directives, Part 1. In particular, the different approval criteria needed for the different types of ISO documents should be noted. This document was drafted in accordance with the editorial rules of the ISO/IEC Directives, Part 2 (see www.iso.org/directives).

Attention is drawn to the possibility that some of the elements of this document may be the subject of patent rights. ISO shall not be held responsible for identifying any or all such patent rights. Details of any patent rights identified during the development of the document will be in the Introduction and/or on the ISO list of patent declarations received (see www.iso.org/patents).

Any trade name used in this document is information given for the convenience of users and does not constitute an endorsement.

For an explanation of the voluntary nature of standards, the meaning of ISO specific terms and expressions related to conformity assessment, as well as information about ISO's adherence to the World Trade Organization (WTO) principles in the Technical Barriers to Trade (TBT) see www.iso.org/iso/foreword.html.

This document was prepared by Technical committee ISO/TC 60, *Gears*, Subcommittee SC 1, *Nomenclature and wormgearing*.

This first edition cancels and replaces ISO/TR 14521:2010, which has been technically revised.

The main changes compared to the previous edition are as follows:

— the orginal Clause 6 which focused on geometry has been deleted and ISO/TR 10828 has been referenced.

Any feedback or questions on this document should be directed to the user's national standards body. A complete listing of these bodies can be found at www.iso.org/members.html.

Introduction

This document was developed for the rating and design of enclosed or open single enveloping worm gears with cylindrical worms, and worm-geared motors having either solid or hollow output shafts.

This document is only applicable when the flanks of the worm wheel teeth are conjugate to those of the worm threads.

The particular shapes of the rack profiles from tip to root do not affect the conjugacy when the worm and worm wheel hobs have the same profiles; thus worm wheels have proper contact with worms and the motions of worm gear pairs are uniform.

This document can apply to wormgearing with cylindrical helicoidal worms as defined in ISO/TR 10828 having the following thread forms: A, C, I, N, K.

Other than those mentioned in the three preceding paragraphs, no restrictions are placed on the manufacturing methods used.

In order to ensure proper mating and because of the many different thread profiles in use, it is generally desirable that worms and worm wheels be supplied by the same manufacturer.

In this document, the permissible torque for a worm gear is limited by considerations of surface stress (conveniently referred to as wear or pitting) or bending stress (referred to as strength) in both worm threads and worm wheel teeth, deflection of worm or thermal limitation.

Consequently, the load capacity of a pair of gears is determined using calculations concerned with all criteria described in the scope and 6.4. The permissible torque on the worm wheel is the least of the calculated values.

Gears — Calculation of load capacity of worm gears

1 Scope

This document specifies formulae for calculating the load capacity of cylindrical worm gears and covers load ratings associated with wear, pitting, worm deflection, tooth breakage and temperature. Scuffing and other failure modes are not covered by this document.

The load rating and design procedures are only valid for tooth surface sliding velocities, $\bar{v}_g$, less than or equal to 25 m/s and contact ratios greater than 2,1. For wear, load rating and design procedures are only valid for tooth surface sliding velocities which are above 0,1 m/s. The rules and recommendations for the dimensioning, lubricants or materials selected by this document only apply to centre distances of 50 mm and larger. For centre distances below 50 mm, method A applies.

The choice of appropriate methods of calculation requires knowledge and experience. This document is intended for use by experienced gear designers who can make informed judgements concerning factors. It is not intended for use by engineers who lack the necessary experience. See 4.7.

WARNING — The geometry of worm gears is complex, therefore the user of this document is encouraged to make sure that a valid working geometry has been established.

2 Normative references

The following documents are referred to in the text in such a way that some or all of their content constitutes requirements of this document. For dated references, only the edition cited applies. For undated references, the latest edition of the referenced document (including any amendments) applies.

ISO 1122-1, *Vocabulary of gear terms — Part 1: Definitions related to geometry*

ISO 1122-2, *Vocabulary of gear terms — Part 2: Definitions related to worm gear geometry*

ISO 6336-6, *Calculation of load capacity of spur and helical gears — Part 6: Calculation of service life under variable load*

DIN 3974-1, *Accuracy of worms and wormgears — Part 1: General bases*

DIN 3974-2, *Accuracy of worms and wormgears — Part 2: Tolerances for individual errors*

3 Terms, definitions and symbols

3.1 Terms and definitions

For the purposes of this document, the terms and definitions given in ISO 1122-1, ISO 1122-2 and the following apply.

ISO and IEC maintain terminological databases for use in standardization at the following addresses:

— ISO Online browsing platform: available at https://www.iso.org/obp

— IEC Electropedia: available at http://www.electropedia.org/

3.1.1
actual gear
worm gear set designed by this document

3.2 Symbols

NOTE Where applicable, the symbols are in accordance with ISO 701.

Table 1 — Symbols for worm gears

Symbols	Description	Unit	Figure	Formula
a	centre distance	mm	Figure 1	
a_1	centre distance of the gear concerned	mm	Figure 1	
a_0, a_1, a_2	oil sump temperature coefficients			(118) to (124)
a_T	centre distance of standard reference gear	mm	Figure 1	
a_V	centre distance of a gear operating or test experiences are available	mm	Table 4	
b_{2H}	effective wheel facewidth	mm		
$b_{2H,std}$	standard effective worm wheel facewidth	mm		(10)
b_{2R}	wheel rim width	mm		(132)
b_H	half Hertzian contact width	mm	Annex D	(D.2)
c_k	coefficient for heat transition coefficient			(133)
c_{oil}	specific heat capacity of the oil (for temperature calculation with spray lubrication)	Ws/(kg.K)		(128)
c_α	proximity value for the viscosity pressure exponent α	m^2/N		(22)/(24)
$d_{a\,1}$	worm tip diameter	mm		(89)
$d_{a\,2}$	worm wheel throat diameter	mm		
$d_{e\,2}$	worm wheel outside diameter	mm		
$\vec{dF}$	force transmitted by a segment of the contact line	N	Figure B.2	(B.3)
dl	length of contact line segment	mm		(B.1) to (B.6)
$d_{f\,1}$	worm root diameter	mm		(104)
$d_{f\,2}$	worm wheel root diameter	mm		(111)
d_{m1}	worm reference diameter	mm		
d_{m2}	worm wheel reference diameter	mm		(41) to (43)
d_{m1T}	reference diameter of the worm, from standard reference gear	mm	Table 4	(44), (45)
d_{m2T}	reference diameter of the wheel, from standard reference gear	mm	Table 4	
$\vec{e}_x$	unit vector pointing in direction of the x-axis	mm		(B.4)
f_h	worm wheel face width factor for the parameter for the minimum mean lubricant film thickness	—		(16)
f_p	worm wheel face width factor for the parameter for the mean Hertzian stress	—		(17)
Δf	relative deviation between a quantity of the gear concerned and a reference gear	—	Figure 1	
Δf_T	relative deviation between the centre distance of the gear concerned and the standard reference gear	—	Figure 1	
Δf_V	relative deviation between the centre distance of the gear concerned and a gear operating or test experiences are available	—	Figure 1	

Table 1 *(continued)*

Symbols	Description	Unit	Figure	Formula
h_{am1}	worm tooth reference addendum in axial section	mm		(86)
h_{min}	minimum lubricant film thickness	µm		(C.1)
$h_{min\ m}$	minimum mean lubricant film thickness	µm		(21)
h^*	parameter for minimum mean lubricant film thickness	—		(14)/(15)
h_T^*	parameter for minimum mean lubricant film thickness of the standard reference gear	—	Table 4	
k	lubricant constant	1/K		(27)/(29)
l_1	spacing of the worm shaft bearings	mm		(103)
l_{11}, l_{12}	bearing spacing of the worm shaft	mm	Figure 5	(103)
$m_{x\,1}$	axial module	mm		
Δm_{lim}	material loss limit	mg		(88)
Δs	tooth thickness loss	mm		(111)
Δs_{lim}	allowable tooth thickness loss	mm		(87)
$\vec{n}$	normal vector			(B.5)
n_1	rotational speed of the worm shaft	min^{-1}		
p_H	Hertzian stress	N/mm^2		(B.1)/(B.6)
p_{Hm}	Hertzian stress; mean value for the total contact area	N/mm^2		(B.7)
p_m^*	parameter for the mean Hertzian stress	—		(11)/(12)/(B.8)
p_{mT}^*	parameter for the mean Hertzian stress of the standard reference gear	—	Table 4	
q_1	diameter quotient	mm		
$\vec{r}$	radius from the axis of the worm wheel to the contact point B	mm		(B.4)
s_{f2}	mean tooth root thickness of the wheel teeth in the spur section	mm		(111)
s_{ft2}	mean tooth root thickness of the wheel teeth in the spur section	mm		(111)
s_{gB}	sliding path of the worm flanks within the Hertzian contact of the wheel flank per number of cycles of the wheel, around the contact point (local value)	mm		(D.3)/(D.5)
s_{gm}	mean sliding path	mm		(D.7)
s_{m2}	tooth thickness at the reference diameter of the worm wheel	mm		(111)
s_K	rim thickness	mm	Figure 6	(113)
s_{Wm}	wear path inside of the required life expectancy	mm		(30)/(D.1)
s_{mx1}	worm tooth thickness in axial section	mm		
s_{mx1}^*	worm tooth thickness in axial section coefficient	—		(111)
s^*	parameter for the mean sliding path	—		(17)/(18)/(D.8)
s_T^*	parameter for the mean sliding path of the standard reference gear	—	Table 4	
Δs	tooth thickness loss			(111)

Table 1 *(continued)*

Symbols	Description	Unit	Figure	Formula
Δs_{lim}	allowable tooth thickness loss			(87)/(111)
$t_{contact}$	time of contact	s		(D.2)
u	gear ratio			(1)
u_T	gear ratio of the standard reference gear		Table 4	
$\vec{v}_1$	velocity of a flank point of the worm	m/s	Figure B.1	
$\vec{v}_2$	velocity of a flank point of a worm wheel	m/s	Figure B.1	
v_{1n}	worm velocity component normal to the contact line	m/s	Figure B.2	
v_{2n}	wheel velocity component normal to the contact line	m/s	Figure B.2	(D.2)
$\vec{v}_{gB}$	sliding velocity normal to the line of contact in flank direction	m/s		(D.3)/(D.5)/(D.6)
v_g	sliding velocity at reference diameter	m/s		(9)/(49)/(50)/(51)/ (H.2)/(H.3)/(H.5)
v_{ref}	reference sliding velocity	m/s		(H.2) to (H.5)
$v_{\Sigma n}$	sum velocity in normal direction	m/s		(11)/(C.4)
x_2	worm wheel profile shift coefficient	—		
z_1	number of threads in worm	—		
z_2	number of teeth in worm wheel	—		
A	coefficient for kinematic viscosity			(33)
A_{fl}	total flank surface of the worm wheel	mm^2		(89)
A_R	dominant cooled surface of the gear set	m^2		(132)
B	coefficient for kinematic viscosity	—		(34)
B	coefficient for h^*	mm		(14)
E_1	modulus of elasticity of the worm	N/mm^2		
E_2	modulus of elasticity of the worm wheel	N/mm^2		
E_{red}	equivalent modulus of elasticity	N/mm^2	Table 4	(20)
F_{xm1}	axial force to the worm shaft	N		(4)/(7)
F_{xm2}	axial force to the worm wheel	N		(3)/(6)
F_{rm1}	radial force to the worm shaft	N		(5)
F_{rm2}	radial force to the worm wheel	N		(11)
F_{tm1}	circumferencial or tangential force to the worm shaft	N		(4)/(6)
F_{tm2}	circumferencial or tangential force to the worm wheel	N		(3)/(7)
dF/dl	specific loading	N/mm		(C.5)
J_{0T}	reference wear intensity	—	Figure 4	(69) to (79)
$J_{0I}, J_{0II}, J_{0III}$	reference wear intensity for stage I, II, III	—		(H.6) to (H.7)
J_W	wear intensity	—		(68)
J_{WP}	wear intensity	—		(H.6)
K_n	rotational speed factor/wheel bulk temperature	—		(135)
$K_{H\alpha}$	transverse load distribution factor	—		6.2.3
$K_{H\beta}$	longitudinal load distribution factor	—		6.2.3
K_S	size factor/wheel bulk temperature	—		(137)

Table 1 *(continued)*

Symbols	Description	Unit	Figure	Formula
K_A	application factor	—		6.2.1
K_v	dynamic factor	—		6.2.2
K_W	lubricant film thickness parameter	—		(80)
K_v	viscosity factor/wheel bulk temperature	—		(136)
K_1	factor	—		(G.5)
L_h	life time	h		
N_L	number of stress cycles of the worm wheel	—		(31)
N_{LI}, N_{LII}, N_{LIII}	number of stress cycles of the worm wheel for stage I to III	—		(H.1)
N_S	number of starts per hour	—		(70)
P_1	input power to the worm shaft	W		
P_2	output power from the worm wheel shaft	W		
P_K	cooling capacity of the oil with spray lubrication	W		(127) (125)
P_V	total power loss of the worm gear unit	W		(38)
P_{V0}	idle running power loss	W		(38)/(39)/(G.1)
$P_{Vz1\text{-}2}$	meshing power loss in reducer	W		(62)
$P_{Vz2\text{-}1}$	meshing power loss in increaser	W		(64)
P_{VD}	sealing power loss	W		(44)/(45)
P_{VLP}	bearing power loss through loading	W		(40) to (43)
Q_{oil}	spray quantity	m^3/s		(127)
Ra_1	arithmetic mean roughness for worm	µm	Table 4	
Ra_T	arithmetic mean roughness for reference gear	µm		(62)
Rz_1	mean roughness depth	µm		7.4.6
S_F	tooth breakage safety factor	—		(106)
$S_{F\,min}$	minimum tooth breakage safety factor	—		(107)
S_H	pitting safety factor	—		(91)
S_{Hmin}	minimum pitting safety factor	—		(92)
S_T	temperature safety factor	—		(115)/(125)
$S_{T\,min}$	minimum temperature safety factor	—		(116)/(126)
S_W	wear safety factor	—		(65)
$S_{W\,min}$	minimum wear safety factor	—		(66)
S_δ	deflection safety factor	—		(101)
$S_{\delta\,min}$	limit of deflection safety factor	—		(102)
T_1	input torque to the worm shaft	Nm		(1)
T_{1N}	nominal input torque to the worm shaft	Nm		(1)
T_2	output torque from the worm wheel	Nm		(2)/(B.4)/(B.5)
T_{2N}	nominal output torque from the worm wheel	Nm		(2)
V_{SUMn}	sum of velocities at contact point			(C.1)
W_H	—			(84)/(85)
W_{ML}	material — lubricant factor	—	Table 7	
W_{NS}	start factor	—		(83)
W_P	damage factor	—		(H.8)
W_S	lubricant structure factor	—		(81)/(82)

Table 1 *(continued)*

Symbols	Description	Unit	Figure	Formula
Y_F	form factor/tooth breakage	—		(110)
Y_G	geometry factor/coefficient of friction	—		(59)/(60)
Y_K	rim thickness factor/tooth breakage	—		(113)
Y_{NL}	life factor/tooth breakage	—	Figure 7 a)/b)	Table 11
Y_R	roughness factor/coefficient of friction	—		(61)/(62)
Y_S	size factor/coefficient of friction	—		(57)/(58)
Y_W	material factor/coefficient of friction	—		
Y_ε	contact factor/tooth breakage	—		(109)
$Y\gamma$	lead factor/tooth breakage	—		(112)
Z_h	life factor/pitting	—		(94)
Z_{oil}	lubricant factor/pitting	—		(100)
Z_S	size factor/pitting	—		(96)/(97)
Z_u	gear ratio factor	—		(98)/(99)
Z_v	velocity factor/pitting	—		(95)
α	pressure viscosity factor	m^2/N		6.6
α_L	heat transition coefficient for immersed wheel teeth	$W/(m^2K)$		(133)
α_n	normal pressure angle	°		
α_0	normal pressure angle			(5), (86)
γ_{m1}	reference lead angle of worm	°		(86)
δ_{lim}	limiting value of deflection	mm		(105)
δ_m	incurred deflection	mm		(103)/(104)
δ_{Wn}	flank loss from wheel through abrasive wear in the normal section	mm		(67)
$\delta_{W\,lim}$	limiting value of flank loss	mm		(90)
$\delta_{W\,lim\,n}$	limiting value of flank loss in normal section	mm		(86) to (88)
η_{ges}	total efficiency in reducer	—		(35)
$\eta_{ges1\text{-}2}$	total efficiency worm driving wheel	—		(35)
$\eta_{ges2\text{-}1}$	total efficiency wheel driving worm	—		(36)
η'_{ges}	total efficiency in increaser	—		(36)
$\eta_{z1\text{-}2}$	gear efficiency in reducer	—		(46)/(63)
$\eta_{z2\text{-}1}$	gear efficiency in increaser	—		(47)/(64)
η_{0M}	dynamic viscosity of lubricant at ambient pressure and wheel bulk temperature	Ns/m^2		(25)/(C.1)
θ	temperature	°C		
$\Delta\theta$	temperature difference between oil sump and worm wheel bulk temperature	°C		(131)
θ_{in}	oil entrance temperature	°C		(129)
θ_0	ambient temperature	°C		
θ_{oil}	spray temperature	°C		(129)
$\Delta\theta_{oil}$	oil temperature difference between input and output cooling system	°C		(129)
θ_M	wheel bulk temperature	°C		(130)/(134)
θ_S	oil sump temperature	°C		(117)/(119)
$\theta_{S\,lim}$	limiting value of oil sump temperature	°C		(115)

Table 1 *(continued)*

Symbols	Description	Unit	Figure	Formula
μ_{0T}	base coefficient of friction	—		(49) to (52)
μ_{zm}	mean tooth coefficient of friction	—		(48)
ν_1	POISSON ratio of the worm	—		(20)
ν_2	POISSON ratio for the worm wheel	—		(20)
ν_θ	kinematic viscosity at oil temperature θ	mm^2/s		(32)
ν_{40}	kinematic viscosity at 40 °C	mm^2/s		(32)
ν_{100}	kinematic viscosity at 100 °C	mm^2/s		
ν_M	kinematic viscosity at wheel bulk temperature	mm^2/s		(25)
ρ_1, ρ_2	local radius of curvature	mm		(B.2)
ρ_{oil}	lubricant density	kg/dm^3		(127)
ρ_g	friction angle for the tooth coefficient of friction			(5)
ρ_{oil15}	lubricant density at 15 °C	kg/dm^3		(25)
ρ_{oilM}	lubricant density at wheel bulk temperature	kg/dm^3		(26)
ρ_{red}	equivalent radius of curvature	mm		(B.2)
ρ_z	friction angle for the tooth coefficient of friction	°		(5)
ρ_{Rad}	material density of the wheel	mg/mm^3	Table 8	(88)
$\sigma_{H\,lim\,T}$	pitting strength	N/mm^2	Table 9	
σ_{Hm}	mean contact stress	N/mm^2		(19) (91)
σ_{HG}	limiting value for the mean contact stress	N/mm^2		(93) (91)
τ_F	shear stress at tooth root	N/mm^2		(108) (106)
$\tau_{F\,lim\,T}$	shear endurance strength	N/mm^2	Table 10	
τ_{FG}	limiting value for shear stress at tooth root	N/mm^2		(114) (106)

4 General consideration

4.1 Worm gear load capacity rating criteria

The load capacity of a worm gear corresponds to the torque (or the power) which can be transmitted without the occurrence of tooth breakage or the appearance of excessive damage on the active flanks of the teeth during the design life of the gearing.

Conditions shown in Table 2 can limit the rated load capacity.

Table 2 — Significant factors affecting failure mode and performance (valid for same gear set)

Influencing factors	Failure modes					Efficiency
	Wear	Pitting	Tooth-breakage	Worm shaft deflection	Scuffing	
Load (Hertzian pressure)	x	x	x	x	x	x
Worm speed	x	x			x	x
Oil viscosity	x	x			x	x
Contact Pattern	x	x	x		x	x
Worm surface waviness and roughness	x	x			x	x

Table 2 *(continued)*

Influencing factors	Failure modes					Efficiency
	Wear	Pitting	Tooth-breakage	Worm shaft deflection	Scuffing	
Oil film shearing value					x	x
Shear stress			x			

NOTE Worm thread breakage can occur as a result of bending fatigue of worm threads but is not covered by this document.

— **wear:** damage usually appears on the tooth flanks of bronze worm wheels and is also influenced by the number of starts per hour;

— **pitting:** this form of damage may appear on the flanks of worm wheel teeth; its development is strongly influenced by the load transmitted and the load-sharing conditions;

— **tooth breakage:** shear failure of worm wheel teeth or worm threads can occur when teeth become thin due to wear or overload;

— **worm shaft deflection:** excessive deformation under load can modify the contact pattern between worm and worm wheel;

— **scuffing:** this form of damage often appears suddenly; it is strongly influenced by transmitted load, sliding velocities and the conditions of lubrication.

Factors such as material properties, meshing conditions, (e.g. contact pattern under load) and lubrication greatly impact Hertzian pressure along the lines of contact.

The different rating criteria are calculated independently and not in combination (see Annex J). For a given worm gear pair, the zone of contact can change with loading. At a steady load, fatigue pits can develop which may subsequently be reduced by wear. This can be followed by further pitting, additional wear or a stable condition.

The load capacity of wormgearing is determined by calculations dealing with permissible stresses for pitting and wear, the deflection in the worm, shafts, and the operating temperature. Excessively high working temperature leads to accelerated degradation of the worm gear lubricant. The permissible torque shall be determined from the lowest value of the calculated load capacity.

4.2 Basis of the method

The calculation methods are partly based on investigations of test gears (see, standard reference gear, 4.4), and partly on application experience. Investigations on test gears are mainly ascertained through varied test conditions and verified through practical experience.

4.3 Concept of absolute and relative parameters

The formulae used for the calculation procedure in this document lead to either an absolute form (calculation with absolute parameters) or to a relative form (calculation with relative parameters).

Absolute parameters: The calculation is used when no specific tests are available. The precision of the gear calculations is improved as the differences concerning geometric dimensions, the operating conditions, material and lubricant, to those taken from the standard reference gears are decreased.

Relative parameters: The calculation offers the possibility to use investigation results in the corresponding calculation process directly. This enables the calculation procedure of the specific results to be adapted.

As the dimensions, materials, lubricants and operating conditions of the gear to be calculated approach those of the standard reference gear or, if the corresponding test gear data is available, the deviation is decreased. Figure 1 shows an example of the influence of the centre distance.

To minimize the deviation between the designed gear and the reference gear (or/and test gear if applicable), care should be taken to minimize the difference between both gears specific characteristics including dimensions, materials, lubrication and operating conditions. The gear being designed has a centre distance of a_1, which is clearly a deviation from that of the standard reference gear a_T. Thus a relative deviation Δf_T is given. Furthermore, test results are available for a gear with a centre distance of a_V. In calibrating the calculation procedure to this centre distance, a deviation of Δf_V is yielded (by linear regression). This deviation is significantly smaller than the deviation Δf_T, since the concerned gear is clearly more similar to the test gear than to the reference gear. Therefore, if possible, the limiting values should be determined from the operating or test experience in which each operating condition (tooth form, material, lubricant, rotational speed, loading, etc.) is as similar as possible to that of the gear in question. In calculating the load capacity or various factors, more methods are allowed (see 4.4).

The use of the calculating procedure requires for each case, a realistic estimation of all influential factors, especially the loading, ambient conditions, damage risk (probability of damage) etc. The recommended minimum safety factors shall be increased accordingly (see Annex I).

For a calculation example, see Annex G.

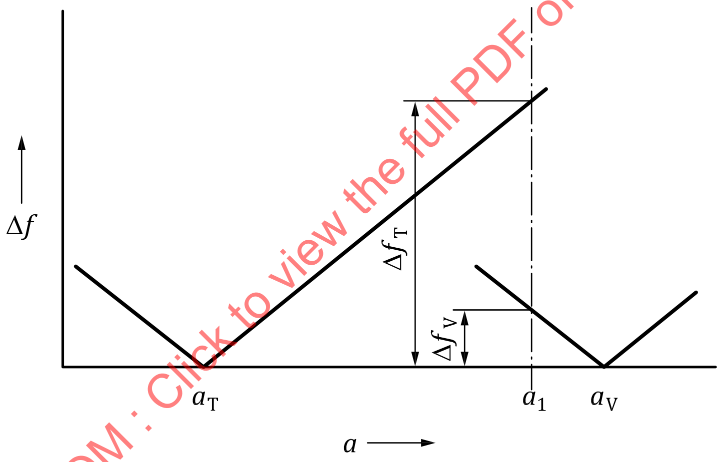

Key

a centre distance

Δf relative deviation between a quantity of the gear concerned and a reference gear

a_1 centre distance of the gear concerned

a_T centre distance of the standard reference gear (see Table 4)

a_V centre distance of a gear operating or test experiences are available

Δf_T relative deviation between the centre distance of the gear concerned and the standard reference gear

Δf_V relative deviation between the centre distance of the gear concerned and a gear operating or test experiences are available

Figure 1 — Deviation as a function of the centre distance (based on linear regression)

4.4 Applicability

The technical information provided in this document is based on the following:

— knowledge and judgement acquired over years of experience in designing, manufacturing and operating wormgearing;

— results of bench testing I-worm gears having centre distances from 65 mm to 160 mm and transmission ratios for 4,8 to 50.

Three methods are provided for the calculation of each parameter:

— method A (the most accurate derived from experimental and measurement data);

— method B (calculated parameters derived using numerical methods);

— method C (approximated methods).

4.5 Validity

The validity for the various parts of the calculating procedure of this document is restricted to conditions where operating experience already exists. If further test results are available, the scope of validity can be extended by calibration with a valid calculation procedure with respect to the type and extent of the additional testing.

The rating and design procedures are valid for the following:

— **flank forms:** A, N, K, I, C according to ISO/TR 10828;

— **worm rotational speed:** up to 5 000 r/min;

— **gear ratio:** from 5 to 100;

— **sliding velocity:** between tooth surfaces from 0,1 m/s to 25 m/s for wear;

— **shaft angle:** of 90°;

— **accuracy grade:** the worm accuracy grade (according to DIN 3974) should be specified to be one accuracy grade better than wheel;

— **worm materials**:

  — case hardened steels, case hardened (HRC = 58 to 62);

  — through hardened steels, flame or induction hardened (HRC = 50 to 56);

  — the calculation procedures are based on experiments carried out with worms made of 16MnCr5 (case hardened), no studies having been carried out for other materials yet. However, in the case of sufficient surface hardness (as above), hardness penetration depth, core hardness and correct heat treatment, the calculation procedures of the above-mentioned materials can be used;

  — other materials and heat treatments (such as nitriding steels, gas nitrided) can be used with sufficient experience in accordance with method A;

— **worm wheel materials:** material and notes based on experience which are as listed in Table 3 should be used;

NOTE Other materials not listed in Table 3 can be used.

— **centre distance**:

  — for temperature calculation (wear, pitting) the range is from 60 mm up to 500 mm centre distance;

  — for other criteria (pitting, tooth breakage) the range is between 50 mm up to 500 mm centre distance.

— **lubricants**:

  — mild additive CLP-oils according to ISO 6743-6;

— compounded oils (steam cylinder oils), no test results available, included as a mineral oil in this document;

— polyglycols;

— polyalphaolefines based on limited test results.

The calculations are based essentially on studies carried out with I-worm gears. The results have been converted to worm gears with other flank forms by means of similarity considerations.

Table 3 — Common worm wheel materials

Worm material	16MnCr5 case hardened					
Wheel material	GZ-CuSn12[a,c]	GZ-CuSn-12Ni2[a]	GC-CuSn-12Ni2	GZ-CuAl-10Ni[a,b]	GJS-400-15	GJL-250
	Bronze	Nickel bronze	Nickel bronze	Aluminium bronze	Spheroidal graphite cast iron	Grey cast iron
Wear	+	+	+	o	o	o
Pitting	+	+	+	o	–	–
Tooth Breakage	+	+	–	+	+	+
Temperature	+	+	+	+	–	–

Key

+ covered study available

o limited study

– empirical values

[a] Bronze should be homogenous and free from blow holes in the gearing region. Average grain size <150 µm. Grain size variation may have a significant influence on the capacity, resulting in variation of 20 % or more, if not maintained consistent. For the determination of grain size, a minimum of 50 grains is needed to be observed on the area of active flanks.

[b] Forged aluminium bronze can be treated like GZ-CuAl10Ni.

[c] Forged phosphor bronze can be treated like GZ-CuSn12.

NOTE 1 See EN 1982, EN 1563 and EN 1561 for the material designation.

NOTE 2 For low sliding velocities, $v_g < 0,5$ m/s.

4.6 System considerations

In this document no attempt is made to address complete drive systems, backdriving, torsional vibrations, critical speeds or other types of vibrations which may affect the operation of worm gears.

4.7 Calculation methods A, B, C

4.7.1 Generality on methods A, B and C

4.7.1.1 General

This document contains influential factors based on research results and operational experiences. The factors are differentiated with reference to:

a) Factors which are concerned with meshing geometry or compatibility shall be calculated using given formulae.

b) Factors which are multi–influenced, or are independent of each other (which do not however affect each other), or both. These include factors which affect an influence on the permitted stress.

The factors can be determined by different methods which are, where necessary, characterised by additional parameters A to C. Method A is more precise than B and so on. It is recommended to use the most precise method. With important operations, the method used should be agreed upon by the manufacturer and the purchaser.

4.7.1.2 Method A

Here the factor is determined through exact measurement, extensive mathematical analysis of the transfer system or existing operational experiences. Because of this, all gear and loading data shall be known.

4.7.1.3 Method B

The factors are determined by a method which, for most applications, is sufficiently precise. The assumptions under which they are developed are stated. In determining a specific factor, the application shall be within the range of the given assumptions.

4.7.1.4 Method C

For some factors additional simplified approximation procedures are specified. The assumptions under which they are developed are stated. In determining a specific factor, the application shall be within the range of the given assumptions.

4.7.2 Notes on numerical formulae

The formulae specified in this document shall be calculated in the specified units (see Table 1).

4.7.3 Base conditions, interaction

— Wear:

This procedure is in accordance with the investigation described in Reference [23] and is based on practical experience.

— Pitting damage:

The procedure follows the investigation described in Reference [30] and takes into consideration practical experience. The Hertzian stress is an essential influencing variable to the physics causing pitting development, in addition to this however, other influences are also of importance e.g. the tangential forces and the effects of slip and roll movement. These additional influences are not considered here, therefore, the limiting value of the load capacity (surface stress values) should be developed through tests on worm gears or through evaluation of relevant operational results. Allowable values, resulting from specimen examination (e.g. disk tests), only allow for relative statements and may only be used for the load capacity calculation if scientific investigation of this manner has been completed.

— Interaction between scuffing and wear:

Short term scuffing incurred by bronze wheels can be "healed". This healing is only possible through wear, however this document does not provide estimations for this wear behaviour.

— Interaction between wear and pitting:

It is known from practical testing that pitting development can be stabilised by increased wear. Pitting can also be stopped through continual wear.

At higher wear intensities, that is when the wear capacity limits the life endurance, pitting is a secondary consideration. Alternatively with higher pitting, wear is not the limiting criteria.

— Interaction between wear and tooth breakage:

The calculation of the tooth breakage factor takes into account that the tooth thickness of the worm wheel is decreased by wear.

4.7.4 Other notes

Calculated load capacities are valid for the following conditions:

— continuous operation,

— constant loading,

— correct alignment,

— the contact area width approaches the full facewidth after running in.

All other loaded conditions are outside the scope of this document.

4.8 Standard reference gear

With certain calculation procedures the absolute calculating formulae are similar to the relative calculating formulae. If the adopted sizes of the corresponding standard reference gear (subscript T) shall be employed, the relative calculating formulae can be transferred to the absolute calculating formulae (see Table 4).

Table 4 — Main data from the standard reference gear

Centre distance a_T	100 mm
Gear ratio u_T	20,5
Worm reference diameter d_{m1T}	36 mm
Worm wheel reference diameter d_{m2T}	164 mm
Parameter for mean Hertzian stress p_{mT}*	0,92 (Formula (53))
Parameter for mean lubricant film thickness h_T*	0,07 (Formula (55))
Parameter for mean sliding path s_T*	30,8 (Formula (59))
Worm material	16MnCr5 case hardened
Wheel material	GZ-CuSn12Ni2
Lubricant density	1,048 kg/dm^3
Flank form	I (ISO/TR 10828)
Normal pressure angle	20°
Worm surface roughness Ra_1	0,5 µm
Equivalent modulus of elasticity E_{red}	150 622 N/mm^2

5 Required date for calculation

5.1 Input variable

For the calculation, the following variables shall be known.

Geometry data:

— Center distance, a

— Effective wheel facewidth, b_{2H}, see ISO/TR 10828:2015, Figure 4

— Wheel rim width, b_{2R}, see ISO/TR 10828:2015, Figure 4

— Reference diameter, d_{m1}, d_{m2}

— Axial module of the worm, m_{x1}

— diameter quotient, q_1

— Number of teeth, z_1, z_2

— Worm wheel profile shift coefficient, x_2

— Normal pressure angle, α_n

— Profile flank form, (A, N, K, I, C)

— Worm wheel outside diameter, d_{e2}

— Rim thickness, s_k, see Figure 6

— Worm tip diameter, d_{a1}

— Worm thread thickness in axial section coefficient, $s_{mx1}{}^*$

— Accuracy grade of pitch deviation by analogy with DIN 3974

— Root diameter d_{f2}

Loading:

— Nominal output torque, T_{2N}

— Application factor, K_A

— Rotational speed of worm, n_1

— Life time, L_h

— Number of start per hour, N_S

In order to calculate the efficiency, the power loss and the wear and pitting safety factors are also necessary:

— Worm and wheel material

— Lubricant data ρ_{oil}, ν_{40}, ν_{100}

— Type of oil: mineral oil/polyglycol

— Type of lubrication: splash or spray lubrication

— Roughness of the worm flanks, Ra_1

— Immersed or not immersed worm wheel

— Type of bearing at the worm: located — non-located bearing; adjusted bearing

— Number of sealing rings at the worm

— Housing with fan or housing without fan

— Ambient temperature, θ_0

To calculate the deflection safety factor:

— Worm bearing spacing, l_1, or l_{11}, l_{12}

5.2 Safety factors

Safety factors (calculated) are differentiated according to wear, S_W, pitting, S_H, deflection, S_δ, tooth breakage, S_F and maximum temperature, S_T. The defined minimum safety factors, S_W, S_H, S_δ, S_F and S_T shall not be reduced below values given in this document.

The safety factors shall be chosen after careful consideration of the following influences:

— how safe are the assumptions of the load concerned;

— how safe are the assumptions of the operating conditions concerned;

— what are the consequences of damage.

Higher safety factors may be agreed between manufacturer and purchaser.

6 Forces, speeds and parameters for the calculation of stresses

6.1 General

For the calculation of load capacity, the following forces, speeds and parameters are required. They are used to describe stress mechanisms for both tooth flank and tooth root.

All forces transferred to the gear shall be compiled as accurately as possible, when calculating the net applied force.

When calculating the tooth forces, both the external and internal influences shall be taken into account in accordance with 6.2.1 and ISO 6336-6.

6.2 Tooth forces

6.2.1 Application factor

The application factor, K_A, shall consider all forces externally introduced to the gear, in addition to the nominal forces described in 6.2.2. These extra forces depend on the driving machine characteristics and driven machine characteristics, the masses and elasticities in the output and drive lines (e.g. from shafts and clutches) and operating conditions. Guide values for K_A can be found in ISO 6336-6. In some circumstances it may be useful to calculate the tooth force components with nominal torque, for example for shaft or bearing calculations, in which case the application factor should be equal to 1 in Formulae (1) and (2).

6.2.2 Dynamic factor

Internal influences are covered by factor K_v.

The measurement of the tooth root stresses at different circumferential velocities (ω_2) has indicated that the amount of internally generated dynamic loads can be neglected ($K_v = 1$).

6.2.3 Load distribution factor

Influences of load distribution are covered by factors $K_{H\beta}$ and $K_{H\alpha}$.

The methods within this document assume that the worm gear has been accurately manufactured and run-in, such that there is an even load distribution over the face width (along the contact lines) and there is an even load distribution over the tooth flanks in mesh ($K_{H\alpha} = K_{H\beta} = 1$).

Variable torque, which results in varying worm deflections, however, may result in non-uniform load distribution along the contact lines with correspondingly increased wear during gear operation. In order to keep this effect to a minimum, a deflection safety factor is required (see Clause 10).

6.2.4 Tooth force components

The torques required for the calculations of the following forces shall be calculated from the nominal input and output torques as follows:

$$T_1 = T_{1\mathrm{N}} \cdot K_\mathrm{A} \tag{1}$$

$$T_2 = T_{2\mathrm{N}} \cdot K_\mathrm{A} \tag{2}$$

The basis for the load capacity calculation is the rated torque of the driven machine, which is the operational torque for the heaviest working conditions. The nominal torque can also be taken from the motor provided that this torque corresponds with the permissible torque of the driven machine. If this is not the case another sensible definition should be chosen.

The tangential, axial and radial forces, $F_{\mathrm{tm}1,2}$, $F_{\mathrm{xm}1,2}$, $F_{\mathrm{rm}1,2}$, acting on the worm and wheel are shown in Figure 2.

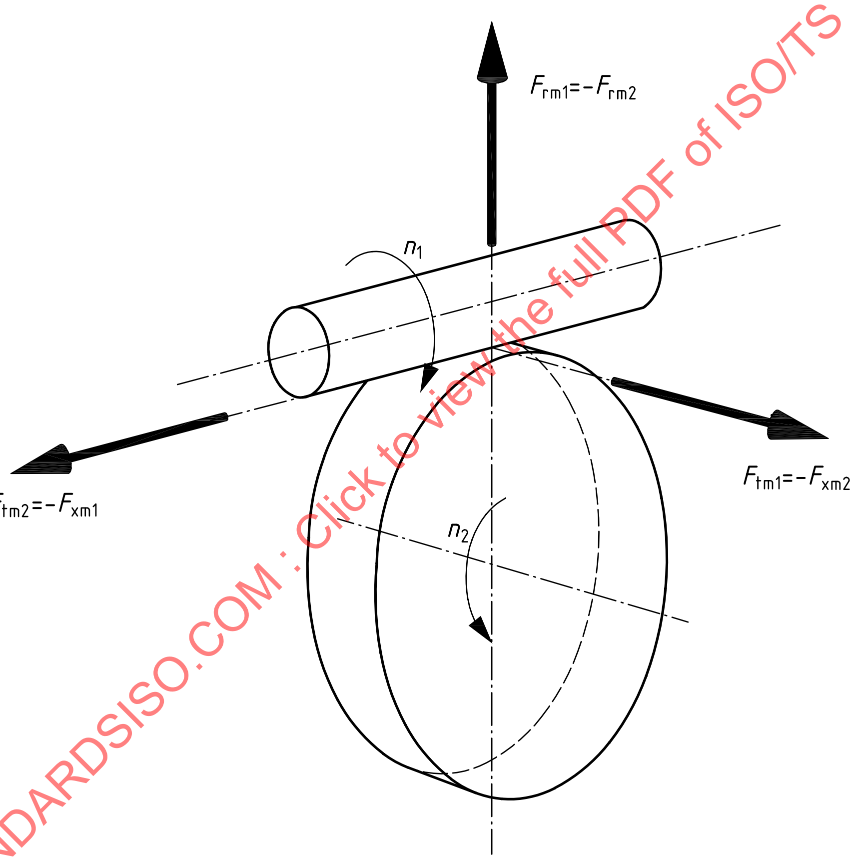

Figure 2 — Tooth load components

Worm driving the worm wheel:

If the calculation of tooth components with nominal torque is required, the application factor effect shall be removed from Formulae (3) to (8).

$$F_{\mathrm{tm}1} = 2\,000 \cdot \frac{T_1}{d_{\mathrm{m}1}} = 2\,000 \cdot \frac{T_2}{d_{\mathrm{m}1} \cdot \eta_{\mathrm{ges}} \cdot u} = -F_{\mathrm{xm}2} \tag{3}$$

$$F_{tm2} = 2\,000 \cdot \frac{T_2}{d_{m2}} = 2\,000 \cdot \frac{T_1 \cdot \eta_{ges} \cdot u}{d_{m2}} = -F_{xm1} \tag{4}$$

with η_{ges} according to Formula (35)

$$F_{rm1} = -F_{rm2} = F_{tm1} \cdot \frac{\tan\alpha_0}{\sin(\gamma_{m1} + \rho_z)} \tag{5}$$

with: $\rho_z = \arctan(\mu_{zm})$

μ_{zm} according to Formula (48)

Worm wheel driving the worm:

$$F_{tm1} = 2\,000 \cdot \frac{T_1}{d_{m1}} = 2\,000 \cdot \frac{T_2 \cdot \eta'_{ges}}{d_{m1} \cdot u} = -F_{xm2} \tag{6}$$

$$F_{tm2} = 2\,000 \cdot \frac{T_2}{d_{m2}} = 2\,000 \cdot \frac{T_1 \cdot u}{d_{m2} \cdot \eta'_{ges}} = -F_{xm1} \tag{7}$$

with η_{ges}' according to Formula (36)

$$F_{rm2} = -F_{rm1} = F_{tm2} \cdot \frac{\tan\alpha_n}{\cos(\gamma_{m1} - \rho_z)} \tag{8}$$

NOTE The relationship between input and output torque can be derived from Formulae (3) and (4) if the worm is driving or Formulae (6) and (7) if the worm is driven.

6.3 Sliding velocity at reference diameter

Due to the mostly large slip components in the circumferential direction, to calculate the load capacity it is sufficient to use the sliding velocity at the reference diameter v_g in flank direction:

$$v_g = \frac{d_{m1} \cdot n_1}{19\,098 \cdot \cos\gamma_{m1}} \tag{9}$$

6.4 Physical parameters

6.4.1 Generality on physical parameters

6.4.1.1 General

In order to judge the capacity of worm gears, three non-dimensional parameters based on the geometry of the gears are defined and called physical parameters. These physical parameters are p_m^*, for the mean Hertzian stress, h^*, for the mean lubricant film thickness, and s^*, for the mean sliding path. Since these physical parameters are dependent only on the geometry of the gears, size, loading and lubricant do not influence them. See Annex A and References [23] and [31] for description of their derivations.

The physical parameters are derived according to methods A, B and C.

NOTE 1 The use of method C does not eliminate the need to check that proper gear mesh occurs.

NOTE 2 A, I, N and K profiles of worms are considered as a unique profile.

NOTE 3 Method C is based on mathematical approximation to established Formulae (11) to (18).

6.4.1.2 Method A

Currently there is no method to derive the physical parameters directly from experimental data or measurement of part dimensions.

6.4.1.3 Method B

The physical parameters are derived using numerical methods; for the basis of these parameters 6.4.2 and 6.4.3 and Annexes B, C, D, E and F shall be used. See also References [31] and [35].

6.4.1.4 Method C

NOTE Solutions for the physical parameters can be obtained through approximation formulae from computer — programming according to References [20], [31] and [35].

The formulae apply to flank form I but can also be used in an approximate manner for tooth forms K, A and N. The approximation formulae for C-worm drives are derived from Reference [24] and from operational experience. The approximation formulae indicated in 6.4.2, 6.4.3 and 6.4.4 shall apply to I-worm drives with $\alpha_n = 18$ to 22°, $x_2 = -0{,}5$ to +1, $h_{am1} + h_{am2} \approx 2 \cdot m_{x1}$, C-worm drives with $\alpha_n = 20$ to 24°, $x_2 = 0$ to +0,5, $h_{am1} + h_{am2} \approx 2 \cdot m_{x1}$ and $\rho/m_n \approx 5$ to 7.

For I — Wormdrive, the approximation formulae shall only be applied when the base diameter is smaller than the root diameter.

The approximation formulae are only valid for a worm wheel facewidth of:

$$b_{2H,std} = m_{x1}\left(\sqrt{q_1^2 - (q_1 - 3)^2} + 1\right) \tag{10}$$

For a smaller worm wheel face width the physical parameters p_m^* and h^* are on the unsafe side. Therefore higher safety factors for wear and pitting shall be used or the physical parameters p_m^* and h^* shall be calculated according Method B.

6.4.2 Parameter for the mean Hertzian stress

6.4.2.1 General

The mean Hertzian stress is a parameter of essential importance to the flank loading (see 4.7.3).

For critical applications (such as cranes, lifts, high precision gear set for rotary table and robotic application), method B is recommended for contact pressure calculation.

6.4.2.2 Parameter for the mean Hertzian stress — Method A

A parameter which describes the complex relationships between Hertzian stress and flank loading cannot be given at the moment.

6.4.2.3 Parameter for the mean Hertzian stress — Method B

The mean Hertzian stress used for the determination of the parameter is calculated by means of a computer program e.g. according to References [20], [31] and [35] under the assumption of the equal Hertzian pressure for all simultaneously meshed contact lines. The procedure is to define the contact and then find the curvature radii at the flanks on specific contact line sections. The Hertzian stress can be derived from equivalent cylinders along the contact lines. In each meshing zone more than one tooth is engaged. The Hertzian contact stress along these contact lines are assumed constant. The mean Hertzian stress p_{Hm}, is thus derived from all Hertzian stresses from all the meshing zones.

The Hertzian stress shall be used in the development of the non-dimensional parameter, p_{m}^{*}. This Hertzian stress parameter is only dependant on the gear tooth geometry and is independent of the modulus of elasticity (E-module), material used and centre distance (size). The parameter, p_{m}^{*}, is used in Formula (19) for the derivation of the mean contact stress σ_{Hm}. For details of calculation of this parameter, Annex B shall be used.

6.4.2.4 Parameter for the mean Hertzian stress — Method C

From calculations according to method B a useful non-dimensional parameter for the mean Hertzian stress, p_{m}^{*} is derived.

For I, N, K, A worm drives:

$$p_{\mathrm{m}}^{*}=0{,}179\,4+0{,}238\,9\cdot\frac{a}{d_{\mathrm{m1}}}+0{,}076\,1\cdot x_2\cdot\left|x_2\right|^{3{,}18}+0{,}053\,6\cdot q_1-0{,}003\,69\cdot z_2 -0{,}011\,36\cdot\alpha_{\mathrm{n}}+44{,}981\,4\cdot\frac{x_2+0{,}005\,657}{z_2}\cdot\left(\frac{z_1}{q_1}\right)^{2{,}687\,2} \tag{11}$$

For C-worm drives:

$$p_{\mathrm{m}}^{*}=0{,}140\,1+0{,}186\,6\cdot\frac{a}{d_{\mathrm{m1}}}+0{,}059\,5\cdot x_2\cdot\left|x_2\right|^{3{,}18}+0{,}041\,9\cdot q_1-0{,}002\,88\cdot z_2 -0{,}008\,9\cdot\alpha_{n}+35{,}141\,7\cdot\frac{x_2+0{,}005\,657}{z_2}\cdot\left(\frac{z_1}{q_1}\right)^{2{,}687\,2} \tag{12}$$

For worm wheel with smaller facewidth than $b_{\mathrm{2H,std}}$, p_{m}^{*} shall be modified with the following formulae:

$$p_{\mathrm{m}}^{*}=p_{\mathrm{m}}^{*}\cdot f_{\mathrm{p}}$$

$$f_p=\frac{14\cdot b_{\mathrm{2H}}^{2}-\left(28\cdot b_{\mathrm{2H,std}}+m_{\mathrm{x1}}\right)\cdot b_{\mathrm{2H}}+300\cdot m_{\mathrm{x1}}^{2}+14\cdot b_{\mathrm{2H,std}}^{2}+b_{\mathrm{2H,std}}\cdot m_{\mathrm{x1}}}{300\cdot m_{\mathrm{x1}}^{2}} \tag{13}$$

This formula is only valid for $(b_{\mathrm{2H,std}} - 2{,}5\ m_{\mathrm{x1}}) \le b_{\mathrm{2H}} \le b_{\mathrm{2H,std}}$.

For smaller value than $(b_{\mathrm{2H,std}} - 2{,}5\ m_{\mathrm{x1}})$, Method B shall be used. For higher value than $b_{\mathrm{2H,std}}$, $f_{\mathrm{p}} = 1$ shall be used.

6.4.3 Parameter for the mean lubricant film thickness

6.4.3.1 General

The mean lubricant film thickness is a parameter of essential importance to the calculation of the flank load capacity and the efficiency.

6.4.3.2 Parameter for the mean lubricant film thickness — Method A

A parameter which describes the complex relationship between changeable lubricant film thickness above the meshing zone and flank loading cannot be given at the moment.

6.4.3.3 Parameter for the mean lubricant film thickness — Method B

The mean minimum lubricant film thickness, $h_{\mathrm{min\ m}}$, is derived by means of computer programming (see References [20], [31] and [35]) based on a method from Dowson and Higginson[17]. The tooth flanks shall be replaced in sections along the specific contact lines by rolling cylinders that are equivalent to the flank curvature. Taking into account the velocity relationships, the Hertzian stress and the lubricant properties, the minimum lubricant film thickness, $h_{\min\,m}$, for specific roll sections can be calculated using Reference [15]. The mean minimum lubricant film thickness can now be found from the mean value of all the minimum lubricant film thicknesses for all contact points. From the minimum mean lubricant film thickness a non-dimensional parameter, $h^{*,}$ for the lubricant film thickness shall be determined. This parameter is only dependant on the gearing geometry. It is independent from centre distance (size), velocity, rate of revolutions, lubricant and loading. The relationship between h^* and $h_{\min\,m}$ is shown by Formula (21). Annex C shall be used for details of calculation.

6.4.3.4 Parameter for the mean lubricant film thickness — Method C

From calculations according to method B, a useful non-dimensional parameter for the mean lubricant film thickness, h^*, is derived.

For I, N, K, A worm drives:

$$\begin{aligned} h^* = {} & -0{,}393 + 2{,}915\,7 \cdot 10^{-6} \cdot (z_2)^{-0{,}084\,7} \cdot \alpha_n^{0{,}059\,5} \cdot \left(7{,}947 \cdot 10^{-7} \cdot x_2 + 5{,}927 \cdot 10^{-5}\right) \\ & \cdot \left((1 - 0{,}038 \cdot q_1) \cdot q_1 + 65{,}576\right) \cdot \left(\left(108{,}854\,7 \cdot \frac{z_1}{q_1} - 1\right) \cdot \frac{z_1}{q_1} - 3\,294{,}921\right) \\ & \cdot \left(\left(3{,}291 \cdot 10^{-3} \cdot B + 1\right) \cdot B - 13\,064{,}58\right) \end{aligned} \tag{14}$$

with $B = \sqrt{6 \cdot m_{x1} \cdot d_{m1} - 9 \cdot (m_{x1})^2} + m_{x1}$

For C-worm drives:

$$\begin{aligned} h^* = {} & -0{,}511 + 3{,}790\,4 \cdot 10^{-6} \cdot (z_2)^{-0{,}084\,7} \cdot \alpha_n^{0{,}059\,5} \cdot \left(7{,}947 \cdot 10^{-7} \cdot x_2 + 5{,}927 \cdot 10^{-5}\right) \\ & \cdot \left((1 - 0{,}038 \cdot q_1) \cdot q_1 + 65{,}576\right) \cdot \left(\left(108{,}854\,7 \cdot \frac{z_1}{q_1} - 1\right) \cdot \frac{z_1}{q_1} - 3\,294{,}921\right) \\ & \cdot \left(\left(3{,}291 \cdot 10^{-3} \cdot B + 1\right) \cdot B - 13\,064{,}58\right) \end{aligned} \tag{15}$$

with $B = \sqrt{6 \cdot m_{x1} \cdot d_{m1} - 9 \cdot (m_{x1})^2} + m_{x1}$

For worm wheel with a smaller facewidth than $b_{2H,std}$, h^*shall be modified with the following formulae:

$$h^* = h^* \cdot f_h$$

$$f_h = \frac{-2 \cdot b_{2H}^2 + \left(4 \cdot b_{2H,std} + m_{x1}\right) \cdot b_{2H} + 75 \cdot m_{x1}^2 - 2 \cdot b_{2H,std}^2 - b_{2H,std} \cdot m_{x1}}{75 \cdot m_{x1}^2} \tag{16}$$

This formulae is only valid for $(b_{2H,std} - 2{,}5\ m_{x1}) \le b_{2H} \le b_{2H,std}$.

For smaller value than $(b_{2H,std} - 2{,}5\ m_{x1})$, Method B shall be used. For higher value than $b_{2H,std}$, $f_h = 1$ shall be used.

6.4.4 Parameter for the mean sliding path

6.4.4.1 General

The sliding path of a contact point of the worm flank within the width of Hertzian flattening is a parameter of essential importance to the flank load.

6.4.4.2 Parameter for the mean sliding path — Method A

A parameter which describes exactly the complex relationship between changeable sliding path above the meshing zone and flank loading cannot be given at the moment.

6.4.4.3 Parameter for the mean sliding path — Method B

The sliding path, s_{gB}, is the sliding path of a point on the worm flank within the width of Hertzian flattening. On the basis of local s_{gB} values, the arithmetical mean value from all contact lines in the meshing zone shall be calculated. This is calculated by computer programming (see References [20], [31] and [35]).

On this basis a non-dimensional parameter, s^*, is defined for the sliding path according to Annex D, which shall be used for details of calculation.

6.4.4.4 Parameter for the mean sliding path — Method C

From calculations according to method B, a useful non-dimensional parameter for the mean sliding path s^* for common dimensions, is derived.

For I, N, K, A worm drives:

$$s^* = 0{,}78 + 0{,}21 \cdot u + 5{,}6 / \tan \gamma_{m1} \tag{17}$$

For C-worm drives:

$$s^* = 0{,}94 + 0{,}25 \cdot u + 6{,}7 / \tan \gamma_{m1} \tag{18}$$

6.5 Calculation of mean contact stress

Mean contact stress σ_{Hm}, corresponding to 6.4.2:

$$\sigma_{Hm} = \frac{4}{\pi} \cdot \left(\frac{p_m^* \cdot T_2 \cdot 10^3 \cdot E_{red}}{a^3} \right)^{0,5} \tag{19}$$

The parameter for mean contact stress p_m^*, shall be derived according to 6.4.2 (method B or C).

Equivalent modulus of elasticity:

$$E_{red} = \frac{2}{\left(1-\nu_1^2\right)/E_1 + \left(1-\nu_2^2\right)/E_2} \tag{20}$$

For different material combinations the modulus of elasticity, Poisson ratio and the equivalent modulus of elasticity, E_{red}, are given in Table 5.

Table 5 — Modulus of elasticity and cross sectional contraction parameter for wheel materials

Wheel material	GZ-CuSn12	GZ-CuSn12Ni2 GC-CuSn12Ni2	GZ-CuAl10Ni	GJS-400-15	GJL-250
	Bronze	Nickel bronze	Aluminium bronze	Spheroidal graphite cast iron	Grey cast iron
E_2 [N/mm^2]	88 300	98 100	122 600	175 000	98 100
ν_2 [-]	0,35	0,35	0,35	0,30	0,30
E_{red} [N/mm^2]	140 114	150 622	174 053	209 790	146 955
NOTE See Reference [33], equivalent modulus of elasticity $E_{red,}$ for the combination with a steel worm (E_1 = 210 000 N/mm^2, ν_1 = 0,3).					

6.6 Calculation of mean lubricant film thickness

With some simplifications according to Annex C (see Reference [15]), the following applies:

$$h_{\text{min m}} = 21 \cdot h^* \cdot \frac{c_\alpha^{0,6} \cdot \eta_{0M}^{0,7} \cdot n_1^{0,7} \cdot a^{1,39} \cdot E_{red}^{0,03}}{T_2^{0,13}} \tag{21}$$

(for units, see Clause 3)

The parameter for the lubricant film thickness h^*, shall be determined in accordance with 6.4.3 (method B or C).

Here, the mostly unknown pressure viscosity exponent, α, shall be replaced by an approximated constant, c_α, which is a function of the oil type:

— for mineral oils or compounded oils:

$$c_\alpha = 1{,}7 \cdot 10^{-8} \quad \text{in} \quad \text{m}^2/\text{N} \tag{22}$$

— for polyalphaolefines:

$$c_\alpha = 1{,}4 \cdot 10^{-8} \quad \text{in} \quad \text{m}^2/\text{N} \tag{23}$$

— for polyglycols:

$$c_\alpha = 1{,}3 \cdot 10^{-8} \quad \text{in} \quad \text{m}^2/\text{N} \tag{24}$$

The dynamic viscosity, η_{0M}, at ambient pressure, p_0, and wheel bulk temperature, θ_M:

$$\eta_{0M} = \nu_M \cdot \rho_{oilM} / 1\,000 \tag{25}$$

The kinematic viscosity, ν_M, can be determined either by Formula (32) or from the viscosity-temperature characteristic line of the lubricant at the wheel bulk temperature θ_M, (see Clause 13 for the determination of the wheel bulk temperature θ_M).

The lubricant density, ρ_{oilM}, at the wheel bulk temperature, θ_M, shall be (see Reference [29]):

$$\rho_{oilM} = \rho_{oil15} / \left(1 + k \cdot (\theta_M - 15)\right) \tag{26}$$

Where ρ_{oil15} is the density of the lubricant at 15 °C (from the data sheet of the oil manufacturer).

Lubricant constant for mineral oils or compounded oils:

$$k = 7{,}0 \cdot 10^{-4} \tag{27}$$

Lubricant constant for polyalphaolefines:

$$k = 7{,}6 \cdot 10^{-4} \tag{28}$$

Lubricant constant for polyglycols:

$$k = 7{,}7 \cdot 10^{-4} \tag{29}$$

6.7 Calculation of the wear path

The wear path s_{Wm} is calculated from the number of stress cycles of the wheel N_L and the sliding path of the worm within the contact zone on the wheel flank:

$$s_{Wm} = s_{gm} \cdot N_L = s^* \cdot \frac{\sigma_{Hm} \cdot a}{E_{red}} \cdot N_L \tag{30}$$

The parameter for the mean sliding path, s^*, shall be determined in accordance with 6.4.4 (methods B or C).

Number of stress cycles of the wheel N_L, for the life expectancy, L_h:

$$N_L = L_h \cdot \frac{n_1 \cdot 60}{u} \tag{31}$$

6.8 Calculation of the lubricant kinematic viscosity

The lubricant kinematic viscosity, ν_θ, for an oil temperature, θ, between 0,1 °C and 100 °C shall be calculated from the kinematic viscosity, ν_{40}, at 40 °C and the kinematic viscosity, ν_{100}, at 100 °C:

$$\nu_\theta = 10^{10^{A \cdot \log(\vartheta + 273) + B}} - 0{,}7 \tag{32}$$

with

$$A = \frac{\log\left(\dfrac{\log(\nu_{40} + 0{,}7)}{\log(\nu_{100} + 0{,}7)}\right)}{\log\left(\dfrac{313}{373}\right)} \tag{33}$$

$$B = \log\left(\log(\nu_{40} + 0{,}7)\right) - A \cdot \log(313) \tag{34}$$

7 Efficiency and power loss

7.1 General

The efficiency or power loss is needed for the calculation of tooth force components and checking of the temperature safety factor (See Annex I).

7.2 Total efficiency

7.2.1 Method A

Determination of the total efficiency from measurements of the total power loss at operating conditions at the actual gear.

7.2.2 Method B

Total efficiency (worm driving wheel):

$$\eta_{ges1-2} = P_2 / (P_2 + P_V) = (P_1 - P_V) / P_1 \tag{35}$$

Total efficiency (wheel driving worm):

$$\eta_{ges2-1} = P_1 / (P_1 + P_V) = (P_2 - P_V) / P_2 \tag{36}$$

The total power loss P_V shall be derived as is stipulated in 7.3 (method B or C).

7.3 Total power loss

7.3.1 Methods of calculation

7.3.1.1 Method A

Measurement of the total power loss at the actual gear.

7.3.1.2 Method B

The total power loss, P_V, shall be calculated as follows:

$$P_V = P_{Vz} + P_{V0} + P_{VLP} + P_{VD} \tag{37}$$

If the relationship between the meshing power loss and the oil sump temperature is known from previous tests, the meshing power loss, P_{Vz}, shall be calculated from the measured oil sump temperature.

The idle running power loss, P_{V0}, cannot, to a satisfactory degree of accuracy, be defined by a simple calculation appropriate to a method B calculation. The dependence on viscosity in particular is the cause of uncertainty. Thus, method C shall be used for the determination of P_{V0}.

The bearing load power losses, P_{VLP}, can be calculated with calculation procedures from the bearing manufacturer.

The sealing power loss, P_{VD}, can be calculated with calculation procedures from the seal manufacturer.

7.3.1.3 Method C

The total power loss, P_V, shall be derived from Formula (37). The derivation of the meshing power loss, P_{Vz}, shall be according to 7.5, the idle running power loss, P_{V0}, shall be according to 7.3.2, the bearing load power loss, P_{VLP}, shall be according to 7.3.3 and the sealing power loss, P_{VD}, shall be according to 7.3.4.

NOTE For more precise calculation on power losses in bearings, seals, ISO/TR 14179-2 can be used.

7.3.2 Idle running power loss

The idle running power loss shall be (see Reference [26]):

$$P_{\mathrm{V0}} = 0{,}89 \cdot 10^{-4} \cdot a \cdot n_1^{4/3} \tag{38}$$

Formula (38) is based on Formula (39):

$$P_{\mathrm{V0}} = 0{,}89 \cdot 10^{-2} \cdot \frac{a}{a_{\mathrm{T}}} \cdot n_1^{4/3} \tag{39}$$

7.3.3 Bearing load power loss

The bearing power loss, P_{VLP}, of a complete gear set due to the bearing load shall be (see Reference [26]):

— For adjusted bearing arrangement with defined axial clearance (such as straddle mounted taper roller bearings):

$$P_{\mathrm{VLP}} = 0{,}03 \cdot P_2 \cdot a^{\,0{,}44} \cdot \frac{u}{d_{\mathrm{m2}}} \tag{40}$$

— For located — non-located bearing arrangement:

$$P_{\mathrm{VLP}} = 0{,}013 \cdot P_2 \cdot a^{\,0{,}44} \cdot \frac{u}{d_{\mathrm{m2}}} \tag{41}$$

Formulae (40) and (41) are based on Formulae (42) and (43):

For an adjusted bearing arrangement:

$$P_{\mathrm{VLP}} = 0{,}028 \cdot P_2 \cdot \left(\frac{a}{a_{\mathrm{T}}}\right)^{0{,}44} \cdot \frac{u}{u_{\mathrm{T}}} \cdot \frac{d_{\mathrm{m2T}}}{d_{\mathrm{m2}}} \tag{42}$$

For a located — non-located bearing arrangement:

$$P_{\mathrm{VLP}} = 0{,}012 \cdot P_2 \cdot \left(\frac{a}{a_{\mathrm{T}}}\right)^{0{,}44} \cdot \frac{u}{u_{\mathrm{T}}} \cdot \frac{d_{\mathrm{m2T}}}{d_{\mathrm{m2}}} \tag{43}$$

For a sliding bearing the power loss can be calculated according to the relevant literature (see Bibliography [35]).

7.3.4 Sealing power loss

For typical applications the following formulae shall be used.

Power loss per lip:

$$P_{\mathrm{VD}} = 11{,}78 \cdot 10^{-6} \cdot d_{\mathrm{m1}}^2 \cdot n_1 \tag{44}$$

Formula (44) is based on Formula (45):

$$P_{\mathrm{VD}} = 15{,}3 \cdot 10^{-3} \cdot \frac{d_{\mathrm{m1}}^2}{d_{\mathrm{m1T}}^2} \cdot n_1 \tag{45}$$

The power loss at the seals on the worm wheel shaft can be neglected.

7.3.5 Adaptation of the calculation procedure to a specific test

In the case where measurements of power losses are available, the above-mentioned calculation procedures can be adapted. The values for the standard reference gears in the formulae shall be replaced by the corresponding test gear values. The constants shall be adapted to these measurements.

7.4 Gear efficiency

7.4.1 Efficiency calculation

7.4.1.1 General

The gear efficiency is needed for the calculation of the meshing power loss, see 7.5.

7.4.1.2 Method A

The gear efficiency is derived from the meshing power loss as stipulated in 7.5, method A.

7.4.1.3 Method B

Determination of the gear efficiency according to the formulae in method C using the total measured total power loss for the corresponding material-lubricant combination in the original housing under operating conditions.

7.4.1.4 Method C

Gear efficiency $\eta_{Z1\text{-}2}$ (worm driving the wheel):

$$\eta_{Z1-2} = \frac{\tan\gamma_{m1}}{\tan(\gamma_{m1} + \arctan\mu_{zm})} \tag{46}$$

Gear efficiency $\eta_{Z2\text{-}1}$ (wheel driving the worm):

$$\eta_{Z2-1} \approx \frac{\tan(\gamma_{m1} - \arctan\mu_{zm})}{\tan\gamma_{m1}} \tag{47}$$

Mean tooth coefficient of friction:

$$\mu_{zm} = \mu_{0T} \cdot Y_S \cdot Y_G \cdot Y_W \cdot Y_R \tag{48}$$

The calculation of the base coefficient of friction, μ_{0T}, shall be according to 7.4.2, the size factor, Y_S, shall be according to 7.4.3, the geometry factor, Y_G, shall be according to 7.4.4, the material factor, Y_W, shall be according to 7.4.5, and the roughness factor, Y_R, shall be according to 7.4.6.

7.4.2 Base coefficient of friction, μ_{0T}, of the standard reference gear

The base coefficient of friction, μ_{0T}, is a function of the oil type. It shall be taken from Figure 3 or derived by the following formulae:

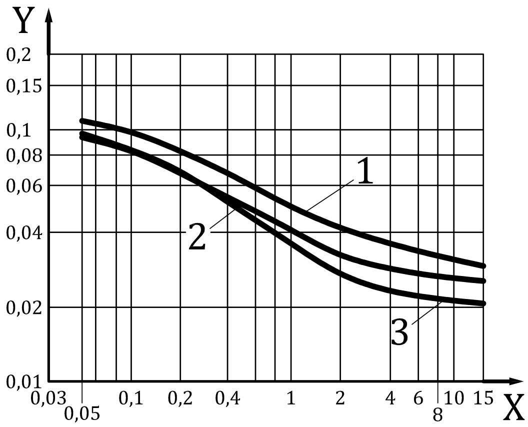

a) All kind of bronze wheels with spray lubrication

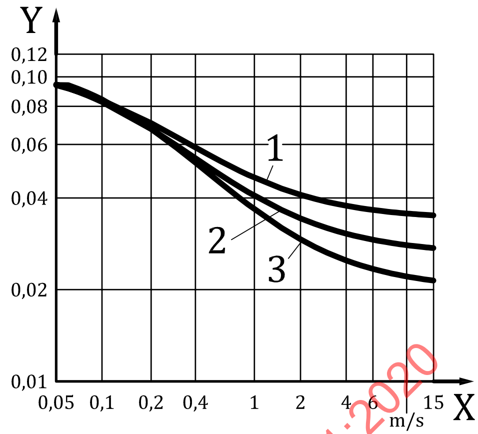

b) All kind of bronze wheels with dip lubrication

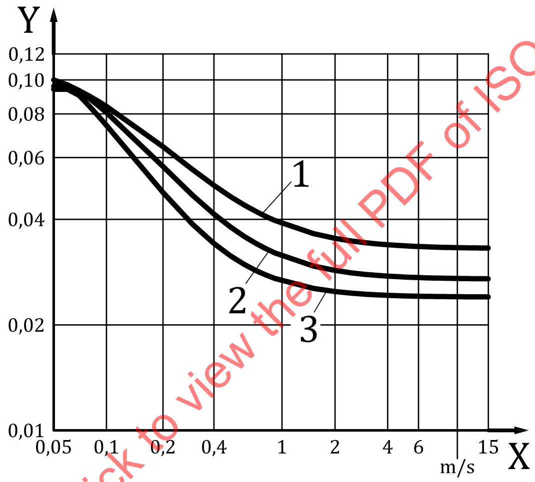

c) Wheels made of grey cast iron

Key

X mean sliding velocity, v_g

Y basic coefficient of friction, μ_{0T}

1 lubrication with mineral oil

2 lubrication with polyalphaolefin

3 lubrication with polyglycol

NOTE Polyglycol with aluminium bronze is not applicable due to chemical incompatibility.

Figure 3 — Base coefficient of friction, μ_{0T}, of the standard reference gear

For bronze wheels, spray lubrication with mineral oil:

$$\mu_{0T} = 0{,}028 + 0{,}026 \cdot \frac{1}{\left(v_g + 0{,}17\right)^{0{,}76}} \le 0{,}1 \tag{49}$$

For bronze wheels, spray lubrication with polyalphaolefin:

$$\mu_{0T} = 0{,}026 + 0{,}017 \cdot \frac{1}{\left(v_g + 0{,}17\right)^{0{,}92}} \le 0{,}096 \tag{50}$$

For bronze wheels, spray lubrication with polyglycol:

$$\mu_{0T} = 0{,}02 + 0{,}02 \cdot \frac{1}{\left(v_g + 0{,}2\right)^{0{,}97}} \le 0{,}094 \tag{51}$$

For bronze wheels, dip lubrication with mineral oil:

$$\mu_{0T} = 0{,}033 + 0{,}007\,9 \cdot \frac{1}{\left(v_g + 0{,}2\right)^{1{,}55}} \le 0{,}1 \tag{52}$$

For bronze wheels, dip lubrication with polyalphaolefin:

$$\mu_{0T} = 0{,}027 + 0{,}005\,6 \cdot \frac{1}{\left(v_g + 0{,}15\right)^{1{,}63}} \le 0{,}096 \tag{53}$$

For bronze wheels, dip lubrication with polyglycol:

$$\mu_{0T} = 0{,}024 + 0{,}003\,2 \cdot \frac{1}{\left(v_g + 0{,}1\right)^{1{,}71}} \le 0{,}094 \tag{54}$$

For grey cast iron wheels, lubrication with mineral oil or polyalphaolefin:

$$\mu_{0T} = 0{,}055 + 0{,}015 \cdot \frac{1}{\left(v_g + 0{,}2\right)^{0{,}87}} \le 0{,}1 \tag{55}$$

For grey cast iron wheels, lubrication with polyglycol:

$$\mu_{0T} = 0{,}034 + 0{,}015 \cdot \frac{1}{\left(v_g + 0{,}19\right)^{0{,}97}} \le 0{,}1 \tag{56}$$

with v_g according to Formula (9).

7.4.3 Size factor

The size factor (see Reference [23]) shall take into account the influence of centre distance:

$$Y_S = 1{,}24 \text{ for } a < 65 \text{ mm} \tag{57}$$

$$Y_S = (100/a)^{0{,}5} \text{ for } 65 \text{ mm} < a < 250 \text{ mm}$$

$$Y_S = 0{,}632 \text{ for } a > 250 \text{ mm}$$

See Annex G for additional information

Formula (57) is based on Formula (58):

$$Y_S = (a_T / a)^{0,5} \tag{58}$$

7.4.4 Geometry factor

The geometry factor (see Reference [23]) shall take in to account the influence of the gear geometry to the lubricant film thickness:

$$Y_G = (0,07 / h^*)^{0,5} \tag{59}$$

with h^* according to 6.4.3.

Formula (59) is based on Formula (60):

$$Y_G = \left(h_T^* / h^*\right)^{0,5} \tag{60}$$

7.4.5 Material factor

The material factor (see Reference [30]) shall take into account the influence of the wheel material, see Table 6.

Table 6 — Material factor Y_W

Wheel material	GZ-CuSn12	GZ-CuSn12Ni2 GC-CuSn12Ni2	GZ-CuAl10Ni	GJS-400-15	GJL-250
	Bronze	Nickel bronze	Aluminium bronze	Spheroidal graphite cast iron	Grey cast iron
Factor Y_W	1,0	0,95	1,1	1,0	1,05

7.4.6 Roughness factor

The roughness factor (see Reference [33]) shall take in to account the influence of the surface roughness of the worm flanks:

$$Y_R = \sqrt[4]{\frac{Ra_1}{0,5}} \tag{61}$$

Formula (61) is based on Formula (62):

$$Y_R = \sqrt[4]{\frac{Ra_1}{Ra_T}} \tag{62}$$

In case the arithmetic mean roughness, Ra_1, of the worm is not known but the mean roughness depth, Rz_1, is, a valid approximation is $Ra_1 = Rz_1/6$.

NOTE The roughness of worm is measured in radial direction of the worm, near the mean cylinder (d_{m1}), according to ISO/TR 10064-4.

7.4.7 Adaptation of the calculation procedure to a specific test

In the case where some of the coefficients of friction are already available (see Reference [28]), the above-mentioned calculation procedures can be adapted. In this case, the values given for the coefficients of friction, μ_{0T}, shall be replaced by the corresponding derived test friction coefficients. The geometry factor, size factor and roughness factor are now valid for the relationship of the practical test gear (subscript T).

7.5 Meshing power loss

7.5.1 Method A

This method is based on the direct measurement of power loss or calculations using a coefficient of friction that was calculated from measurements on similar gears (see Reference [28]).

7.5.2 Method B

Determination of the meshing power loss from the measured total power loss for the corresponding material-lubricant combinations in the original housing under operating conditions minus the losses according to 7.3.

7.5.3 Method C

Derivation from the gear efficiency. Meshing power loss, $P_{\mathrm{Vz1\text{-}2}}$, with the worm driving the worm wheel:

$$P_{\mathrm{Vz1-2}} \approx \frac{0{,}1 \cdot T_2 \cdot n_1}{u} \cdot \left(\frac{1}{\eta_{\mathrm{Z1-2}}} - 1 \right) \tag{63}$$

with $\eta_{\mathrm{Z1\text{-}2}}$ according to Formula (46).

Meshing power loss, $P_{\mathrm{Vz2\text{-}1}}$, with the wheel driving the worm:

$$P_{\mathrm{Vz2-1}} \approx \frac{0{,}1 \cdot T_2 \cdot n_1}{u} \cdot \left(\frac{1}{\eta_{\mathrm{Z2-1}}} - 1 \right) \tag{64}$$

with $\eta_{\mathrm{z2\text{-}1}}$ according to Formula (47).

8 Wear load capacity

8.1 General

Through wear, i.e. continual mass loss, the tooth thickness is decreased. With increasing wear, the danger of one of the safety limits stated in 8.4 being violated also increases. In most danger is the part with the lowest flank hardness, usually the wheel flanks.

8.2 Wear safety factor

The following method assumes that the contact area width approaches the full facewidth after running in. Wear load capacity method is independent of the pitting capacity without consideration of any correlation.

The safety against wear shall be defined as follows:

$$S_{\mathrm{W}} = \delta_{\mathrm{W\,lim\,n}} / \delta_{\mathrm{Wn}} \geq S_{\mathrm{W\,min}} \tag{65}$$

The limiting flank loss, $\delta_{\mathrm{W\,lim\,n}}$, shall be according to 8.4, the expected wear (flank loss in normal δ_{Wn}) shall be according to 8.3.

Minimum safety factor:

$$S_{\mathrm{W\,min}} = 1{,}1 \tag{66}$$

It may be necessary for C worm drives to use a higher minimum safety factor.

8.3 Expected wear

8.3.1 Method A

Direct measurements of gear sets under operating conditions resulting in a realistic estimation of the wear process.

8.3.2 Methods B, C

In calculating the flank loss, δ_{Wn}, the physical parameters, p_{m}^*, h^* and s^*, are required. These shall be calculated as stipulated in 6.4.2 (p_{m}^*), 6.4.3 (h^*) and 6.4.4 (s^*).

The following procedure describing the derivation of δ_{Wn} is based on extensive tests (see Reference [23]). In principle this procedure only applies to the material-lubricant combinations that were tested, and even for these combinations a scatter factor of 2 is normal for the wear. For the combinations not listed, the procedure can only provide a rough approximation. See Annex E for further notes on this procedure.

Flank loss due to wear, δ_{Wn}, of the wheel flank in the normal plane:

$$\delta_{\mathrm{Wn}} = J_{\mathrm{W}} \cdot s_{\mathrm{Wm}} \tag{67}$$

The wear path, s_{Wm}, shall be calculated with Formulae (30) to (31) and the wear intensity, J_{W}, with Formula (68) . The material–lubricant factor, W_{ML}, shall be according to Table 7 and takes into account the influence of the combined effects of the wheel material and lubricant to the wear behaviour (see References [26] and [27]).

Wear intensity, J_{W}:

$$J_{\mathrm{W}} = J_{\mathrm{OT}} \cdot W_{\mathrm{ML}} \cdot W_{\mathrm{NS}} \tag{68}$$

The reference wear intensity, J_{OT}, shall be as given in or derived by Formulae (69) to (79) (see Figure 4).

For bronze wheels, spray lubrication with additive mineral oil:

$$J_{OT} = 2{,}4 \cdot 10^{-11} \cdot K_W^{-3{,}1} \leq 400 \cdot 10^{-9} \quad (69)$$

For bronze wheels, spray lubrication with polyalphaolefines:

$$J_{OT} = 318 \cdot 10^{-12} \cdot K_W^{-2{,}24} \quad (70)$$

For bronze wheels, spray lubrication with polyglycol:

$$J_{OT} = 127 \cdot 10^{-12} \cdot K_W^{-2{,}24} \quad (71)$$

For bronze wheels, dip lubrication with additive mineral oil:

$$J_{OT} = 6{,}5 \cdot 10^{-11} \cdot K_W^{-2{,}68} \leq 400 \cdot 10^{-9} \quad (72)$$

For bronze wheels, dip lubrication with polyalphaolefin:

$$J_{OT} = 558 \cdot 10^{-12} \cdot K_W^{-1{,}91} \quad (73)$$

For bronze wheels, dip lubrication with polyglycol:

$$J_{OT} = 223 \cdot 10^{-12} \cdot K_W^{-1{,}91} \quad (74)$$

NOTE For Formulae (75) to (79) either spray or dip lubrication can be applied.

For aluminium bronze wheels, lubrication with additive mineral oil:

$$J_{OT} = 5{,}45 \cdot 10^{-9} \cdot K_W^{-1{,}23} \leq 400 \cdot 10^{-9} \quad (75)$$

For aluminium bronze wheels, lubrication with polyalphaolefin:

$$J_{OT} = 16{,}6 \cdot 10^{-9} \cdot K_W^{-1{,}17} \quad (76)$$

For grey cast iron wheels, lubrication with additive mineral oil:

$$J_{OT} = 0{,}09 \cdot 10^{-9} \cdot K_W^{-3{,}7} \leq 400 \cdot 10^{-9} \quad (77)$$

For grey cast iron wheels, lubrication with polyalphaolefin:

$$J_{OT} = 0{,}09 \cdot 10^{-9} \cdot K_W^{-3{,}7} \leq 400 \cdot 10^{-9} \quad (78)$$

For grey cast iron wheels, lubrication with polyglycol:

$$J_{OT} = 0{,}58 \cdot 10^{-9} \cdot K_W^{-1{,}58} \quad (79)$$

NOTE Mild additive means small amount of additive.

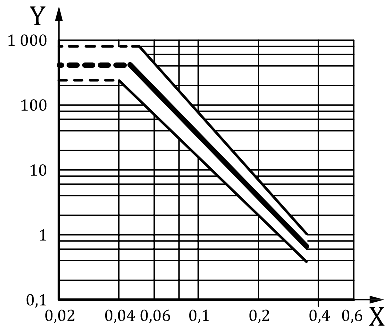

a) Bronze, spray lubrication with additive mineral oil

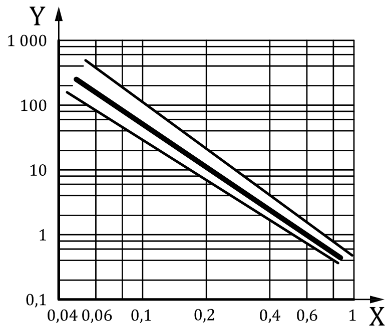

b) Bronze, spray lubrication with polyalphaolefin

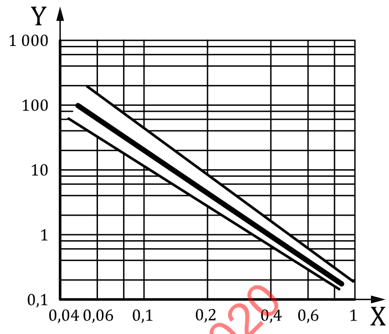

c) Bronze, spray lubrication with polyglycol

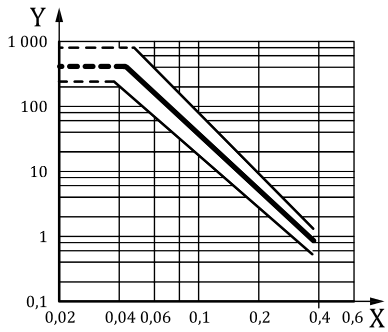

d) Bronze, dip lubrication with additive mineral oil

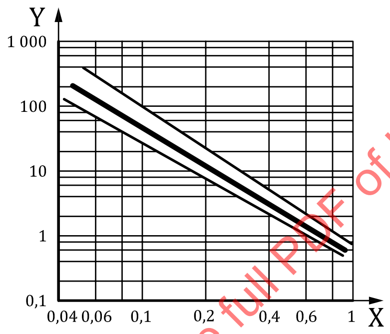

e) Bronze, dip lubrication with polyalphaolefin

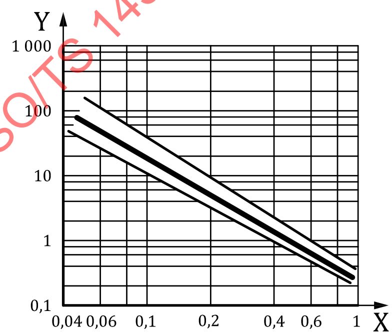

f) For grey cast iron wheels, lubrication with mineral oil or polyalphaolefin

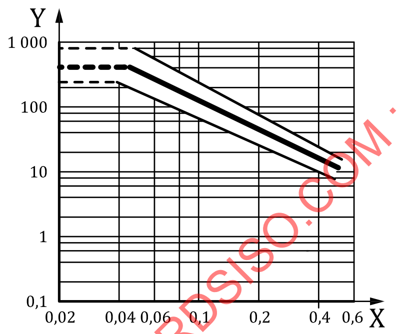

g) Aluminium bronze, lubrication with additive mineral oil

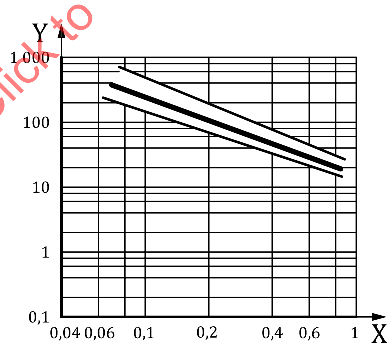

h) Aluminium bronze, lubrication with polyalphaolefin

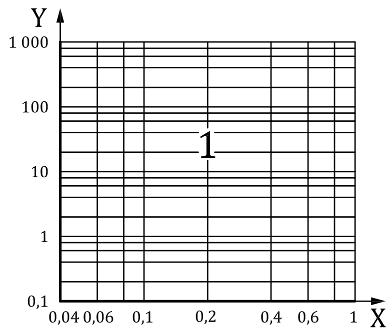

i) Aluminium bronze, lubrication with polyglycol

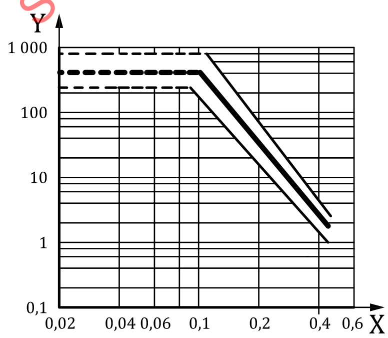

j) Grey cast iron, lubrication with additive mineral oil

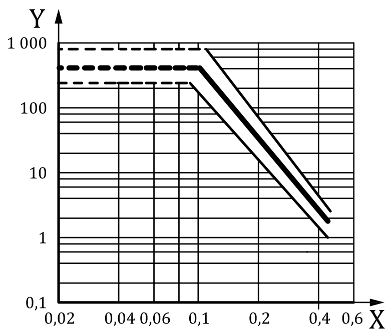

k) Grey cast iron, lubrication with polyalphaolefin

Key

X film thickness parameter, K_W

Y basic wear intensity, J_{0T}, in $\frac{\text{mm wear}}{\text{mm path}}$

1 no data available for the moment

Figure 4 — Basic wear intensity for wheel

Parameter K_W:

$$K_W = h_{\min m} \cdot W_S \cdot W_H \tag{80}$$

The mean lubricant film thickness, $h_{\min m}$, shall be calculated with Formula (21).

For mineral oil, experiments result in a lubricant structure factor of:

$$W_S = 1 \tag{81}$$

For polyglycol and polyalphaolefines:

$$W_S = \frac{1}{\eta_{0M}^{0,35}} \tag{82}$$

The dynamic viscosity, η_{0M}, [Formula (25)] shall be taken at ambient pressure, p_0, and wheel bulk temperature, θ_M. The calculation of $h_{\min m}$ requires the wheel bulk temperature see Clause 13.

As the lubricant film thickness and the lubricant structure factor W_S, are strongly influenced by the wheel bulk temperature, the latter shall be calculated by a method which is as sophisticated as possible (see Clause 13).

The following shall be observed:

If other materials or lubricants are used, tests shall be run, if possible, in order to estimate the effects. The results of any calculations in compliance with this document can only be taken as a guide.

Table 7 — Material/lubricant factor W_{ML}

Worm: 16MnCr5 Case Hardened		Material-lubricant factor W_{ML}		
Wheel material		Mineral Oil	Polyalphaolefine PAO	Polyglycol
GZ-CuSn12Ni2	Nickel bronze	1,0[a]	1[a]	1,75[b]
GC-CuSn12Ni2	Nickel bronze	4,1	4, 1	4,1
GZ-CuSn12	Bronze	1,6[a]	1,6[a]	2,25[a]
GZ-CuAl10Ni	Aluminium bronze	1,0[c]	1,0	—[d]
GGG 40	Spheroidal graphite cast iron	1,0[a]	1,0[a]	1,0[a]
GG 25	Grey cast iron	1,0[a]	1,0[a]	1,0[a]

[a] Scatter zone ±25 %.

[b] Scatter zone ±30 %.

[c] Only valid for $h_{\min m} < 0{,}07$ µm; for $h_{\min m} \geq 0{,}07$ µm; $J_W \cong$ const. = $600 \cdot 10^{-9}$.

[d] Not applicable due to chemical incompatibility.

The start factor, W_{NS}, shall take into account the influence of the number of starts per hour, N_S, on the wear rate (see Reference [25]):

$$W_{NS} = 1 + 0{,}015 \cdot N_S \tag{83}$$

For bronze materials, the pressure factor, W_H, shall be (see Reference [28]):

$$W_H = 1 \text{ for } \sigma_{Hm} < 450 \text{ N/mm}^2$$

$$W_H = \left(\frac{450}{\sigma_{Hm}}\right)^{4,5} \text{ for } \sigma_{Hm} \geq 450 \text{ N/mm}^2 \tag{84}$$

For grey cast iron materials, the pressure factor, W_H, shall be (see Reference [25]):

$$W_H = \left(\frac{300}{\sigma_{Hm}}\right)^{1,4} \tag{85}$$

8.4 Permissible wear

The permissible wear can be set by criteria a) to d). Criteria a) and b) state a limiting value of flank loss, $\delta_{W\,lim}$, which under no circumstances shall be exceeded as this leads to tooth failure. In criterion a), the wear leads to a pointed wheel tooth head, and further wear leads to decreased tooth height. From here the wear increases rapidly. In criterion b), the wear leads to a weakening of the tooth and eventually to tooth breakage.

a) The wheel teeth shall not be permitted to become pointed. This provides the limiting value for the permissible wear. The maximum limiting value, $\delta_{W\,lim}$, for wear is therefore equal to the tooth thickness at the worm wheel throat diameter in the normal section. Based on the tooth thickness at the worm wheel reference diameter the tooth thickness at the worm wheel throat diameter shall be estimated by using a typical tooth addendum $h_{am1} = m_{x1}$

$$\delta_{W\,lim\,n} = m_{x1} \cdot \cos\gamma_{m1} \cdot \left(\pi \cdot \left(1 - s^*_{mx1}\right) - 2 \cdot \tan\alpha_0\right) \tag{86}$$

b) The tooth breakage safety factor, $S_{F\,min}$, can be the limiting wear condition after the required running time. To this end the following is valid:

$$\delta_{W\,lim\,n} = \Delta s_{lim} \cdot \cos\gamma_{m1} \tag{87}$$

where Δs_{lim} is the allowable tooth thickness loss.

For the tooth thickness loss in the axis, Δs_{lim}, the same value as in Formula (111) shall be taken.

c) The material loss, Δm_{lim}, should not exceed a pre-set limit (dependant on oil change intervals and bearing lubrication):

$$\delta_{W\,lim\,n} = \frac{\Delta m_{lim}}{A_{fl} \cdot \rho_{Rad}} \tag{88}$$

with total tooth flank surface A_{fl}:

$$A_{fl} \approx \frac{z_2 \cdot 2m_{x1} \cdot d_{m1} \cdot \arcsin\left(b_{2H}/d_{a1}\right)}{\cos\gamma_{m1} \cdot \cos\alpha_0} \tag{89}$$

Wheel material density, ρ_{Rad}, shall be according to Table 8. See Reference [30].

Table 8 — Wheel material density

Wheel material	GZ-CuSn12	GZ-CuSn12Ni2 GC-CuSn12Ni2	GZ-CuAl10Ni	GJS-400-15	GJL-250
	Bronze	Nickel bronze	Aluminium bronze	Spheroidal graphite cast iron	Grey cast iron
ρ_{Rad} [mg/mm^3]	8,8	8,8	7,4	7,0	7,0

d) The limiting value of flank loss in normal section results from a permissible value for the backlash. Frequently a limit of $\delta_{W\,lim} \cong 0,3 \cdot m_{x1}$ shall be used.

$$\delta_{W\,lim\,n} = 0,3 \cdot m_{x1} \cdot \cos\gamma_{m1} \tag{90}$$

8.5 Adaptation of the calculation procedure to a specific test

The relationships described by Formulae (69) to (79) or Figure 2 for wear intensity were derived by tests with the standard reference gear and by tests with other gears. If test results are available for the gearing (or application) to be calculated, the calculation procedure can be calibrated by the relationship between J_{0T} and the parameter $K_W = h_{min\,m} \times W_S$. The test conditions should be as similar as possible to the operating conditions of the application, for instance the gear ratio, size etc. of the test gears should be as close to the corresponding values of the application.

If the flank loss through wear, δ_{Wn}, of a specific test is known, the reference wear intensity to be calculated, J_{0T}, shall be derived from Formulae (69) and (79). From Formula (69) to (79) a constant can be determined (e.g. $2,4 \cdot 10^{-11}$ for Formula (69)) which is probably more accurate for the application than the constant in Formulae (69) to (79).

9 Surface durability (pitting resistance)

9.1 General

The tooth flanks can be damaged and eventually destroyed by pitting. The highest danger is to the flanks of the part with the lowest hardness, i.e. the wheel flanks.

Pitting can result in the occurrence of wear.

9.2 Pitting safety factor

Pitting safety factor shall be defined as follows:

$$S_H = \sigma_{HG} / \sigma_{Hm} \geq S_{H\,min} \tag{91}$$

The mean actual contact stress, σ_{Hm}, shall be according to 9.3, the limiting contact stress σ_{HG}, shall be according to 9.4.

Minimum safety factor:

$$S_{H\,min} = 1,0 \tag{92}$$

If it results in a safety factor $S_H < 2$, the approach describe in Annex H should be used to check the service life of the gear unit.

It may be necessary for C worm drives to use a higher minimum safety factor.

NOTE For critical applications see 6.4.2.3.

The safety factor concerning the transferable torque shall be equal to the square of S_H (e.g. if S_H = 1,5 the torque safety is 2,25).

9.3 Actual contact stress

9.3.1 Method A

The exact calculation of the relevant contact stress for pitting load capacity is not possible at the moment.

9.3.2 Methods B, C

The mean contact stress, σ_{Hm}, shall be used as a load parameter. It shall be calculated using Formula (19) and the parameter for the mean Hertzian stress, p_m^*, shall be according to 6.4.2 method B or C.

9.4 Limiting value of contact stress

$$\sigma_{HG} = \sigma_{H\,lim\,T} \cdot Z_h \cdot Z_v \cdot Z_s \cdot Z_u \cdot Z_{oil} \qquad (93)$$

Values for pitting resistance for contact stress, $\sigma_{H\,lim\,T}$, shall be according to Table 9. See Reference [30].

Table 9 — Pitting resistance for contact stress

Wheel material	GZ-CuSn12	GZ-CuSn12Ni2 GC-CuSn12Ni2	GZ-CuAl10Ni	GGG-40	GG-25
	Bronze	Nickel bronze	Aluminium bronze	Spheroidal graphite cast iron	Grey cast iron
$\sigma_{H\,lim\,T}$ [N/mm^2]	425	520	660[a]	490[a]	350[a]

[a] For low sliding velocities, v_g < 0,5 m/s.

NOTE The given endurance limits for contact stress are valid for pitting areas accounting for approximately 50 % of the wheel tooth flank.

Life factor:

$$Z_h = (25\,000 / L_h)^{1/6} \le 1,6 \qquad (94)$$

The life time, L_h, shall be applied in hours.

Velocity factor:

$$Z_v = \sqrt{\frac{5}{4 + v_g}} \qquad (95)$$

The sliding velocity at the reference diameter shall be determined from Formula (9).

Size factor:

$$Z_s = \sqrt{\frac{3\,000}{2\,900 + a}} \tag{96}$$

Formula (96) is based on Formula (97):

$$Z_s = \sqrt{\frac{30}{29 + a\ \ /a_T}} \tag{97}$$

Gear ratio factor:

$$Z_u = \left(\frac{u}{20{,}5}\right)^{\frac{1}{6}} \text{ for } u < 20{,}5 \tag{98}$$

$$Z_u = 1 \text{ for } u \geq 20{,}5$$

Formula (98) is based on Formula (99):

$$Z_u = \left(\frac{u}{u_T}\right)^{\frac{1}{6}} \text{ for } u < 20{,}5 \tag{99}$$

$$Z_u = 1 \text{ for } u \geq 20{,}5$$

Lubricant factor:

$$Z_{oil} = 1{,}0 \text{ for polyglycols} \tag{100}$$

Z_{oil} = 0,94 for polyalphaolefines

Z_{oil} = 0,89 for mineral oils

9.5 Adaptation of the calculation procedure to specific test

If test results are available which approach the endurance limits for contact stress, the above calculation procedures can be modified as follows. The given values for contact stress endurance limits $\sigma_{H\ lim\ T}$, shall be replaced by the pitting area parameters derived from operational tests. The size factor and gear ratio factor are thus valid for the behaviour of the test gear (subscript T).

In this case for a_T and u_T the values of the test gear shall be used. See Annex G.

10 Deflection

10.1 General

Excessive or continuously changing deflections of the worm shaft result in meshing interferences that can lead to increased wear.

10.2 Deflection safety factor

The deflection safety factor is:

$$S_\delta = \delta_{lim} / \delta_m \geq S_{\delta min} \tag{101}$$

The limiting value for deflection, δ_{lim}, is defined in 10.4, the actual deflection, δ_m, is defined in 10.3.

Minimum safety factor:

$$S_{\delta min} = 1{,}0 \tag{102}$$

The safety factor concerning torque is equal to the deflection safety factor, S_δ.

10.3 Actual deflection

10.3.1 Method A

Measurement of the deflection of the worm shaft in the housing with the specified bearing.

10.3.2 Method B

Accurate calculation of the deflection of the worm shaft, such as taking account of the centering effect of taper roller bearings, by means of detailed analysis e.g. finite element methods.

10.3.3 Method C

Deflection of the worm:

$$\delta_m = 3{,}2 \cdot 10^{-5} \cdot l_{11}^2 \cdot l_{12}^2 \cdot F_{tm2} \frac{\sqrt{\tan^2(\gamma_{m1} + \arctan \mu_{zm}) + \tan^2 \alpha_0 / \cos^2 \gamma_{m1}}}{\left(1.1 \cdot d_{f1}\right)^4 \cdot l_1} \tag{103}$$

NOTE Formula (103) considers an equivalent uniform diameter for the worm.

The bearing spacing, l_1, l_{11} and l_{12}, are shown in Figure 5:

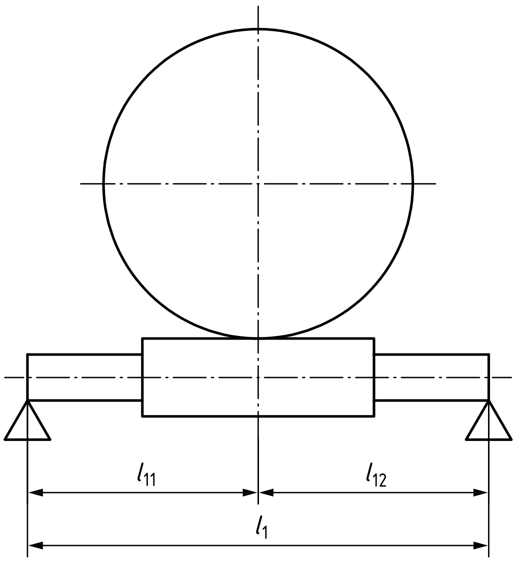

Figure 5 — Bearing spacing

For symmetrical bearing spacing ($l_{11} = l_{12}$), the resultant deflection can be estimated (see Reference [30]):

$$\delta_m = 2 \cdot 10^{-6} \cdot l_1^3 \cdot F_{tm2} \frac{\sqrt{\tan^2(\gamma_{m1} + \arctan \mu_{zm}) + \tan^2 \alpha_0 / \cos^2 \gamma_{m1}}}{(1{,}1 \cdot d_{f1})^4} \quad (104)$$

NOTE Formulae (103) and (104) only take into account the loads due to the gear mesh on the worm shaft. If additional loadings (due to pulley, etc.) are present on the worm shaft these need to be added.

10.4 Limiting value of deflection

In accordance with operating experience, the limiting value of deflection shall be:

$$\delta_{lim} = 0{,}04 \sqrt{m_{x1}} \quad (105)$$

11 Tooth root strength

11.1 Safety factor for tooth breakage

The worm wheel teeth can be plastically deformed or broken as a result of a high tooth root stress.

The safety factor for fatigue breakage shall be:

$$S_F = \tau_{FG} / \tau_F \geq S_{F\,min} \quad (106)$$

The nominal shear stress, τ_F, shall be according to 11.2, the limiting nominal shear stress, τ_{FG}, according to 11.3.

Minimum safety factor:

$$S_{F\,min} = 1{,}1 \quad (107)$$

NOTE The safety for torque is equal to that for fatigue breakage, S_F.

11.2 Actual tooth root stress

11.2.1 Method A

Determination of the tooth root stress through direct measurement of the stresses in the tooth with the aid of strain gauges.

11.2.2 Method B

Determination of the tooth root stress by calculation in accordance with finite element methods.

11.2.3 Method C

This calculation method is based on a nominal shear stress assumption, see Reference [22]. The tooth form factor, Y_F, shall take into account the bending stress component.

Nominal shear stress at the tooth root, τ_F:

$$\tau_F = \frac{F_{tm2}}{b_{2H} \cdot m_{x1}} \cdot Y_\varepsilon \cdot Y_F \cdot Y_\gamma \cdot Y_K \tag{108}$$

The form factor, Y_F, shall be according to Formula (110), the lead factor, Y_γ, according to Formula (112) and the rim thickness factor, Y_K, according to Formula (113).

Contact factor

The contact factor, Y_ε, shall take into account the load distribution to all simultaneously meshed teeth.

$$Y_\varepsilon = 0{,}5 \tag{109}$$

Form factor

The form factor, Y_F, shall take into account the load distribution over the face width, especially the excess load in the region of the wheel face sides and the load increase due to wear at the tooth roots.

$$Y_F = 2{,}9 \cdot m_{x1} / s_{ft2} \tag{110}$$

Mean tooth root thickness

Mean tooth root thickness of the wheel tooth in the mid plane section shall be determined without backlash:

$$s_{ft2} = 1{,}06 \cdot s_{f2} \tag{111}$$

with: $s_{f2} = s_{m2} - \Delta s + (d_{m2} - d_{f2}) \cdot \tan\alpha_0 / \cos\gamma_{m1}$

with: $s_{m2} \approx p_{x1} \cdot \left(1 - s^*_{mx1}\right)$

where Δs is the tooth root thickness loss through wear during the required life expectancy.

Lead factor

Even after the running in, the load distribution along the facewidth of the wheel is not uniform. This effect shall be taken into account by the lead factor, Y_γ.

$$Y_\gamma = 1/\cos\gamma_{m1} \tag{112}$$

Rim thickness factor

The rim thickness factor, Y_K, shall take into account the influence of the rim thickness, s_K, (see Figure 6 for rim thickness):

$$Y_K = 1{,}0 \text{ for } s_K / m_{x1} \geq 2{,}0 \tag{113}$$

$$Y_K = 1{,}043 \ln\left(5{,}218 \cdot \frac{m_{x1}}{s_k}\right) \text{ for } 1{,}0 \leq s_K / m_{x1} < 2{,}0$$

Case with s_K less than $1 \cdot m_{x1}$ shall be avoided.

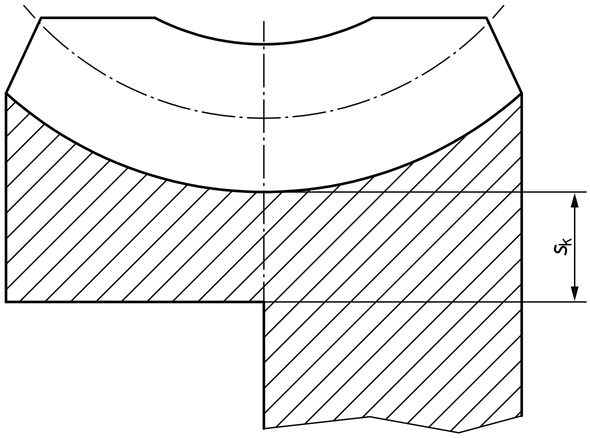

Figure 6 — Rim thickness, s_K, of worm wheel, used to determine the values of Y_K

11.3 Limiting value of shear stress at tooth root

11.3.1 General

Limiting value of shear stress at tooth root:

$$\tau_{FG} = \tau_{F\,lim\,T} \cdot Y_{NL} \tag{114}$$

The shear stress endurance limit, $\tau_{F\,lim\,T}$, shall be according to 11.3.2 and the life factor, Y_{NL}, according to 11.3.3 which takes account of increased load capacity with respect to creep. Here higher plastic deformations can be expected due to permissible accuracy grade deterioration.

11.3.2 Shear endurance limit, $\tau_{F\,lim\,T}$

The mean strength endurance values are shown in Table 10 for bronzes and cast irons. For bronzes, good structures as specified in Table 3 are assumed. When accuracy grade deterioration is not accepted, reduced values should be used, since bronze materials show small plastic deformations. See Annex F.

Table 10 — Mean endurance limits, $\tau_{F\,lim\,T}$, for various worm wheel materials

Wheel material	GZ-CuSn12	GZ-CuSn12Ni2 GC-CuSn12Ni2	GZ-CuAl10Ni	GJS-400-15	GJL-250
	Bronze	Nickel bronze	Aluminium bronze	Spheroidal graphite cast iron	Grey cast iron
Shear endurance limit, $\tau_{F\,lim\,T}$	92	100	128	115	70
Reduced shear endurance limit, $\tau_{F\,lim\,T}$, when accuracy grade deterioration is not accepted	82	90	120	115	70

11.3.3 Life factor, Y_{NL}

For worm wheels of initial accuracy grade up to 7, the life factor, Y_{NL}, as a function of wheel material and the permissible accuracy grade deterioration can be taken from Figure 7 or calculated using the formulae shown in Table 11. Plastic deformation leads to a decrease in the gear wheel accuracy grade. The manufacturer's experience should be considered for wheel qualities better than accuracy grade 7.

The life factor, Y_{NL}, is given numerically in Table 11.

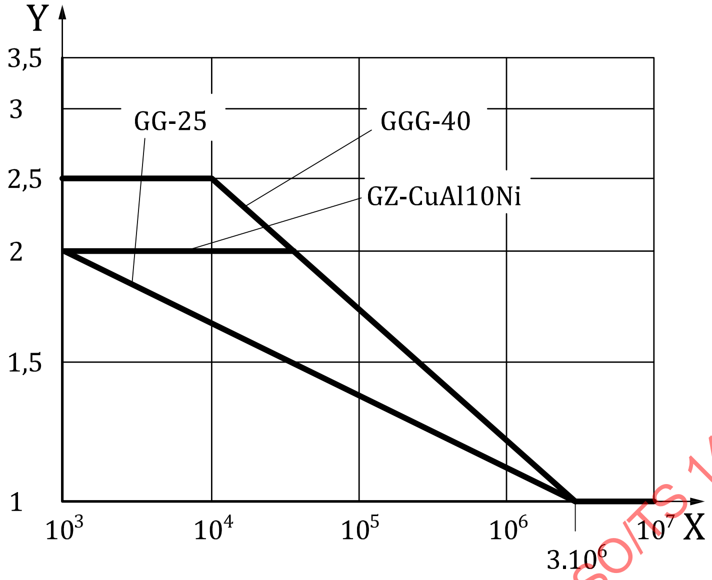

a) Life factor, Y_{NL}, in accordance with experiments: different materials

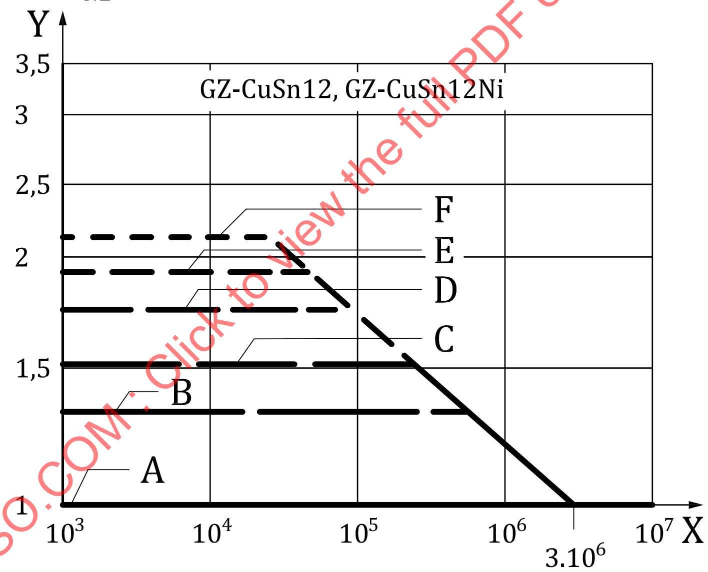

b) Life factor, Y_{NL}, in accordance with experiments: copper-tin-bronze, with deterioration according to accuracy grade 7 to 12 (by analogy with DIN 3974) on pitch deviation

Key

X number of stress cycles at the worm wheel, N_L

Y life factor, Y_{NL}

A deterioration to initial accuracy grade up to 7

B deterioration to accuracy grade 8

C deterioration to accuracy grade 9

D deterioration to accuracy grade 10

E deterioration to accuracy grade 11

F deterioration to accuracy grade 12

Figure 7 — Life factor, Y_{NL}

Table 11 — Life factor as a function of the number of stress cycles, N_L, the material and the permissible accuracy grade

Life Factor Y_{NL}	No. of stress cycles N_L [a]	Material/Accuracy grade
1,25	$<8,3 \cdot 10^5$	GZ-CuSn12 and
$(3 \cdot 10^6/N_L)^{0,16}$	$8,3 \cdot 10^5 \leq N_L \leq 3 \cdot 10^6$	GZ-CuSn12Ni2 with deterioration
1,0	$>3,0 \cdot 10^6$	according accuracy grade DIN 8
1,5	$< 2,3 \cdot 10^5$	GZ-CuSn12 and
$(3 \cdot 10^6/N_L)^{0,16}$	$2,3 \cdot 10^5 \leq N_L \leq 3 \cdot 10^6$	GZ-CuSn12Ni2 with deterioration
1,0	$>3,0 \cdot 10^6$	according accuracy grade DIN 9
1,75	$<9,5 \cdot 10^4$	GZ-CuSn12 and
$(3 \cdot 10^6/N_L)^{0,16}$	$9,5 \cdot 10^4 \leq N_L \leq 3 \cdot 10^6$	GZ-CuSn12Ni2 with deterioration
1,0	$>3,0 \cdot 10^6$	according accuracy grade DIN 10
2,0	$<4 \cdot 10^4$	GZ-CuSn12 and
$(3 \cdot 10^6/N_L)^{0,16}$	$4 \cdot 10^4 \leq N_L \leq 3 \cdot 10^6$	GZ-CuSn12Ni2 with deterioration
1,0	$>3,0 \cdot 10^6$	according accuracy grade DIN 11,
2,5	$<1 \cdot 10^4$	GZ-CuSn12 and
$(3 \cdot 10^6/N_L)^{0,16}$	$1 \cdot 10^4 \leq N_L \leq 3 \cdot 10^6$	GZ-CuSn12Ni2 with deterioration
1,0	$>3,0 \cdot 10^6$	according accuracy grade DIN 12,
2,0	$<4,0 \cdot 10^4$	GZ-CuAl10 Ni
$(3 \cdot 10^6/N_L)^{0,16}$	$4,0 \cdot 10^4 \leq N_L \leq 3 \cdot 10^6$	
1,0	$>3,0 \cdot 10^6$	
2,5	$<1,0 \cdot 10^4$	GGG-40
$(3 \cdot 10^6/N_L)^{0,16}$	$1,0 \cdot 10^4 \leq N_L \leq 3 \cdot 10^6$	
1,0	$>3,0 \cdot 10^6$	
2,0	$<1,0 \cdot 10^3$	GG-25
$(3 \cdot 10^6/N_L)^{0,09}$	$1,0 \cdot 10^3 \leq N_L \leq 3 \cdot 10^6$	
1,0	$>3,0 \cdot 10^6$	

[a] Number of stress cycles of worm wheel, N_L, see Formula (31).

11.4 Adaptation of the calculation procedure to a specific test

If investigations have been carried out, the values given in Table 10 can be replaced by the specific investigation values. The test results give the transferable torque as the damage limit. From this, limiting values for the nominal shear stress, τ_{FG}, shall be derived according to Formula (108).

12 Temperature safety factor

12.1 Temperature safety factor for splash lubrication

12.1.1 General

With increasing temperatures, the life expectancy of the lubricant decreases rapidly. The additive decomposition is accelerated and the sealing rings could be damaged.

The operating temperature of a gear unit is dependent on both the losses and housing design; therefore, these calculations are intended as a guide to be used only when better data is not available.

The temperature safety factor shall be defined as follows:

$$S_T = \theta_{Slim} / \theta_S \geq S_{Tmin} \tag{115}$$

The oil sump temperature, θ_S, shall be according to 12.1.2 and the limiting oil sump temperature, θ_{Slim}, according to 12.1.3.

Minimum safety factor:

$$S_{Tmin} = 1{,}1 \tag{116}$$

12.1.2 Determination of oil sump temperature

12.1.2.1 Method A

Measurement of the oil sump temperature, θ_S, at operating conditions (see Reference [21]).

12.1.2.2 Method B

Accurate thermodynamic analysis of the temperature during operation (see Reference [21]).

12.1.2.3 Method C

Usage limitations:

— centre distance from a = 63 mm to a = 400 mm

— rotational speeds from n_1 = 60 min^{-1} to n_1 = 3 000 min^{-1}

— gear ratio u = 10 to u = 40

— well ribbed housing made out of cast iron.

The oil sump temperature can be estimated as follows:

The use of these approximate formulae for determining sump oil temperature may result in a calculated temperature variation of ±10 °C or even greater.

$$\theta_S = \theta_0 + \left(a_1 \cdot \frac{T_2}{\left(\frac{a}{63}\right)^3} + a_0 \right) \cdot a_2 \tag{117}$$

Oil sump temperature coefficients, a_1 a_0 for housings with fan:

$$a_1 = \frac{3{,}9}{100} \cdot \left(\frac{n_1}{60} + 2 \right)^{0{,}34} \cdot \left(\frac{\nu_{40}}{100} \right)^{-0{,}17} \cdot u^{-0{,}22} \cdot (a - 48)^{0{,}34} \tag{118}$$

$$a_0 = \frac{8{,}1}{100} \cdot \left(\frac{n_1}{60} - 0{,}23 \right)^{0{,}7} \cdot \left(\frac{\nu_{40}}{100} \right)^{0{,}41} \cdot (a + 32)^{0{,}63} \tag{119}$$

Oil sump temperature coefficients, a_1 a_0 for housings without fan:

$$a_1 = \frac{3{,}4}{100} \cdot \left(\frac{n_1}{60} + 0{,}22 \right)^{0{,}43} \cdot \left(10{,}8 - \frac{\nu_{40}}{100} \right)^{-0{,}063\,6} \cdot u^{-0{,}18} \cdot (a - 20{,}4)^{0{,}26} \tag{120}$$

$$a_0 = \frac{5,23}{100} \cdot \left(\frac{n_1}{60} + 0,28\right)^{0,68} \cdot \left(\left|\frac{\nu_{40}}{100} - 2,203\right|\right)^{0,023\,7} \cdot (a + 22,36)^{0,915} \tag{121}$$

Factor a_2 for mineral oils:

$$a_2 = 1 + \frac{9}{(0,012 \cdot u + 0,092) \cdot n_1^{0,5} - 0,745 \cdot u + 82,877} \tag{122}$$

Factor a_2 for polyalphaolefines:

$$a_2 = 1 + \frac{5}{(0,012 \cdot u + 0,092) \cdot n_1^{0,5} - 0,745 \cdot u + 82,877} \tag{123}$$

Factor a_2 for polyglycols:

$$a_2 = 1 \tag{124}$$

12.1.3 Limiting values

The limiting values from the oil manufacturer should be considered for the oil sump temperature.

The following data is usually valid and shall be used when specific data is not available:

— for mineral oil $\theta_{\text{Slim}} \cong 90$ °C,

— for polyalphaolefines $\theta_{\text{Slim}} \cong 100$ °C

— for polyglycols $\theta_{\text{Slim}} \cong 100$ °C to 120 °C. (100 °C is preferred)

12.2 Temperature safety factor for oil spray lubrication

12.2.1 General

The temperature safety factor for spray lubrication shall be:

$$S_T = P_K / P_V \geq S_{\text{Tmin}} \tag{125}$$

The total power loss, P_V, shall be according to 7.3.

Minimum safety factor:

$$S_{\text{Tmin}} = 1,1 \tag{126}$$

12.2.2 Cooling capacity P_K

12.2.2.1 Method A

Measurement of the cooling capacity P_K, at operating conditions (see Reference [21]).

12.2.2.2 Method B

Accurate thermodynamic analysis of the cooling capacity, from entrance and exit temperature, during operation (see Reference [21]).

12.2.2.3 Method C

Cooling capacity:

$$P_K = c_{oil} \cdot \rho_{oil} \cdot Q_{oil} \cdot \Delta\theta_{oil} \quad (127)$$

where, ρ_{oil}, is provided by manufacturer of the oil.

Usual specific heat capacity:

The usual specific heat capacity, c_{oil}, for all type of oils shall be:

$$c_{oil} = 1{,}9 \cdot 10^3 \text{ in Ws/(kg}\cdot\text{K)} \quad (128)$$

Temperature difference:

The temperature difference, $\Delta\theta_{oil}$, of the difference between exit and entrance temperature of the oil.

See Figure 8.

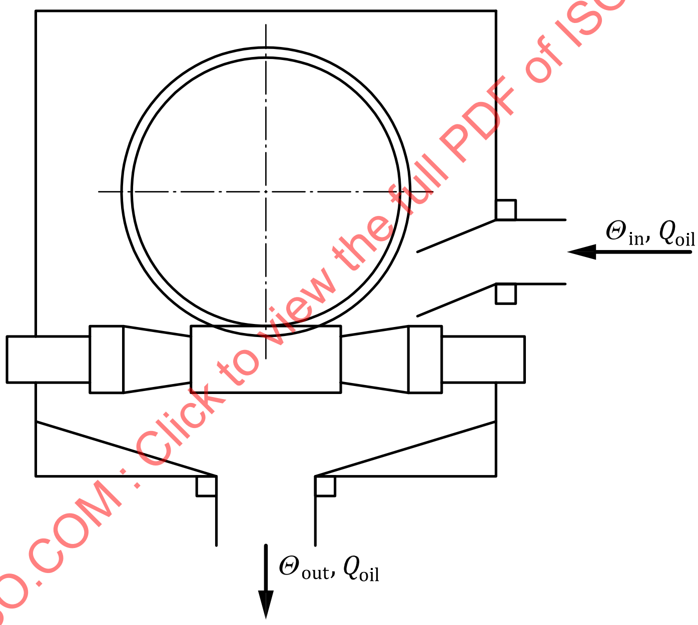

Figure 8 — Definition for cooling capacity

$$\Delta\theta_{oil} = \theta_{out} - \theta_{in} \quad (129)$$

Q_{oil} and $\Delta\theta_{oil}$ shall be agreed upon in co-operation with the manufacturer of the lubricating system.

$\Delta\theta_{oil}$ without cooler 3 °C to 5 °C, with cooler 10 °C to 20 °C.

13 Determination of the wheel bulk temperature

13.1 Wheel bulk temperature with splash lubrication

13.1.1 General

The wheel bulk temperature is required for determination of the wear intensity (see Clause 4).

13.1.2 Method A

Measurement of the wheel bulk temperature at operating conditions.

13.1.3 Method B

Accurate thermodynamic analysis of the wheel bulk temperature at operating conditions.

13.1.4 Method C

Calculation of the wheel bulk temperature, see Reference [23]:

$$\theta_M = \theta_S + \Delta\theta \tag{130}$$

The oil sump temperature, θ_S, shall be according to 12.1.2.

Calculation of the wheel tooth temperature in excess of the oil sump temperature:

$$\Delta\theta = \frac{1}{\alpha_L \cdot A_R} \cdot P_{Vz} \tag{131}$$

The meshing power loss, P_{Vz}, shall be derived according to Formula (63).

Dominant cooled surface of the gear set, A_R:

$$A_R = b_{2R} \cdot d_{m2} \cdot 10^{-6} \tag{132}$$

Heat transition coefficient α_L:

$$\begin{aligned} &\alpha_L = c_K \cdot (1\,940 + 15 \cdot n_1) \text{ for } n_1 \geq 150 \text{ min}^{-1} \\ &\alpha_L = c_K \cdot 4\,190 \text{ for } n_1 < 150 \text{ min}^{-1} \end{aligned} \tag{133}$$

where

c_K = 1 for immersed worm wheel;

c_K = 0,8 for not immersed worm wheel.

13.2 Wheel bulk temperature with spray lubrication

13.2.1 General

The wheel bulk temperature is required for determination of the wear intensity (see Clause 4).

13.2.2 Method A

Measurement of the wheel bulk temperature at operating conditions.

13.2.3 Method B

Accurate thermodynamic analysis of the wheel bulk temperature at operating conditions.

13.2.4 Method C

Calculation of the wheel bulk temperature, see Reference [23]:

$$\theta_M = \theta_{oil} + 16 \cdot K_n \cdot K_v \cdot K_S \cdot P_{Vz} / 1\,000 \tag{134}$$

Rotational speed factor K_n:

$$K_n = (u \cdot 72{,}5 / n_1)^{0{,}35} \text{ for } n_1 \geq 150 \text{ min}^{-1}$$
$$K_n = (u \cdot 72{,}5 / 150)^{0{,}35} \text{ for } n_1 < 150 \text{ min}^{-1} \tag{135}$$

Viscosity factor K_v:

$$K_v = (\nu_E / 55)^{0{,}35} \tag{136}$$

The kinematic viscosity ν_E shall be determined by Formula (32) or from the viscosity-temperature characteristic line of the lubricant at the spray temperature, θ_{oil}.

Size factor K_S:

$$K_S = (160 / a)^{0{,}6} \tag{137}$$

Meshing power loss, P_{Vz}, from 7.5.

Annex A
(informative)

Notes on physical parameters

The research into the causes for worm wheel damage has not yet been sufficiently developed in order to be able to include all the factors in a calculation for the load capacity. This applies especially to the wear load capacity and the surface durability (pitting). Parameters are used for the assessment of the load capacity (e.g. mean contact stress for surface durability). Other influential factors such as coefficient of friction, velocity and size of slip, etc. cannot yet be directly included in the calculation of load capacity.

Despite these deficiencies the parameters are useful when describing the worm drive behaviour, as the limiting values are determined on the basis of running tests with worm gear sets.

With present day computers it is possible to calculate a maximum value for the Hertzian stress in place of the mean value. This maximum value only acts at one contact point. Finite element methods of today allow calculations such as those required to solve contact problems. These programs are also applicable to considerations such as the shear stresses and the stresses induced by increased flank temperature.

This clearly shows that gear optimisation by calculating the load capacity based on these parameters can only be used in a limited manner and that caution is advised.

Annex B
(normative)

Methods for the determination of the parameters

Due to the complex geometrical conditions, it is not possible to give a complete general solution, e.g. for the Hertzian stress of a worm drive. The parameters for the calculation of contact lines can be determined by means of computational calculation. Approximate solutions can also be used for these parameters. Briefly outlined here is the procedure for the calculation of the parameters with the aid of a computer program according to References [31] and [35].

With the formulae for the generatrix of the worm flanks, i.e. for flank form I the transverse involute and the contact lines of the worm and worm wheel are initially calculated. For this purpose, the initial position of a worm tooth is sought. Subsequently the worm is rotated by a defined angle, until no contact between the worm tooth and wheel exists. In general, about 24 worm positions are sufficient. Thus the total range of contact is accounted for and Figure D.2 shows the development of the contact lines as an example.

For each contact point (in general about 2 000 to 3 000) the following parameters shall be calculated:

— the velocities (sum of two surface velocities, sliding velocity etc.);

— Hertzian stress and reduced radius of curvature in compliance with References [31] and [35] for example;

— lubricant film thickness in compliance with the EHL (Elasto Hydrodynamic Lubrication) theory;

— local sliding path. As a rule, it is sufficient to determine a mean parameter for the total meshing zone.

This contact line belongs to a certain position of the worm and to a certain position of the worm wheel. While turning worm and worm wheel, this contact line moves on the worm wheel. For analysing the behaviour of the contact between worm wheel and worm along the contact line, it is useful to divide the contact line into infinitesimal pieces, as indicated in Figure B.1.

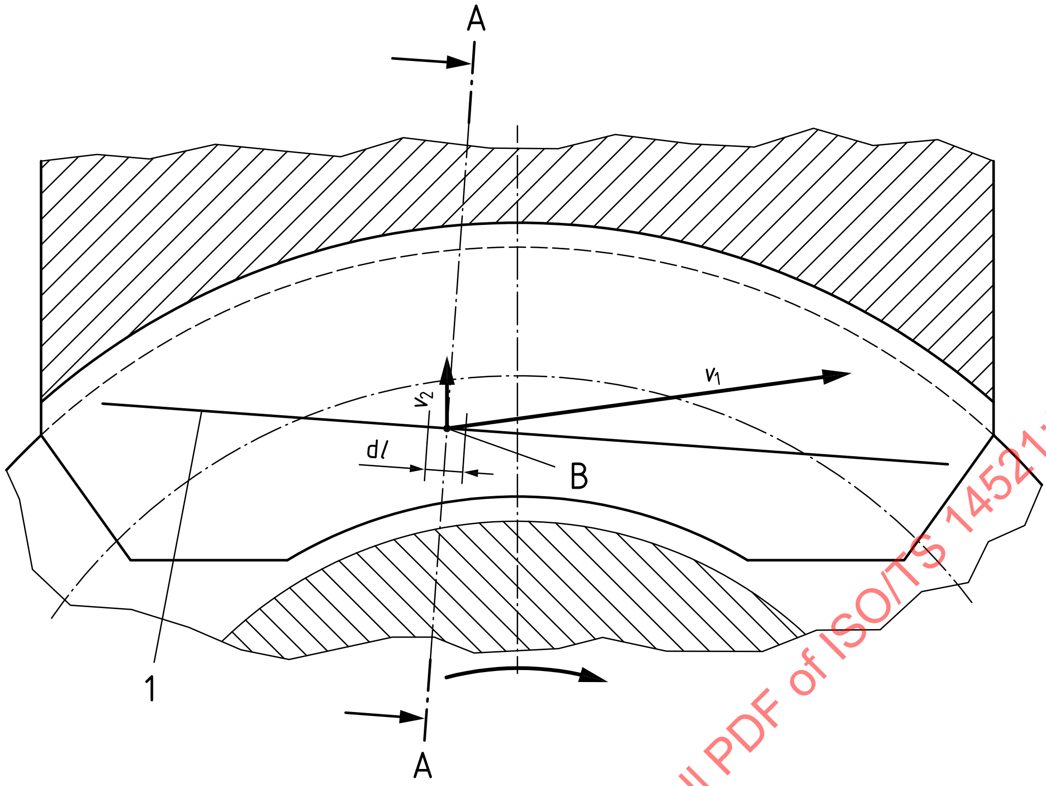

Key

1 contact line

Figure B.1 — Contact line on a worm wheel

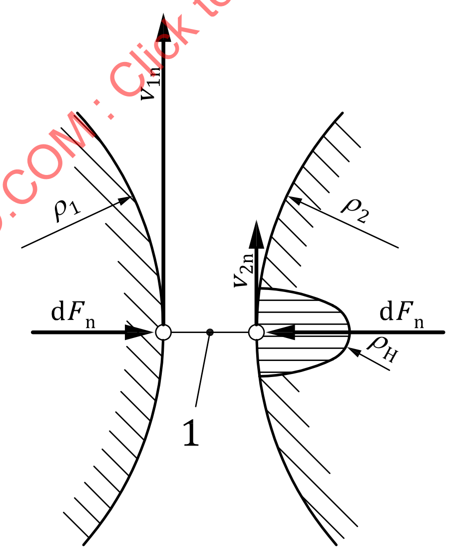

Key

1 contact line

Figure B.2 — Section normal to contact line (section A-A)

Taking one of these pieces of the contact line and looking at a plane normal to this contact line, it is possible to see the flanks of worm and worm wheel as shown in Figure B.2. In contact point B, the main radii of curvature, ρ_1 and ρ_2, of worm and worm wheel can be determined. As a first approximation the actual profile lines of worm and worm wheel can be built by equivalent cylinders with the radii of curvature, ρ_1 and ρ_2. These radii of curvature are important for the calculation of the Hertzian stress along this piece of the contact line. It is also possible to calculate the speeds of the flanks, v_1 and v_2, of the worm and the worm wheel in the contact point B. The knowledge of these speeds is important in order to calculate the lubricant film thickness along this piece of the contact line. The calculation of the speeds takes place in a tangential plane, that touches the flank of the worm as well as the flank of the worm wheel. The Hertzian stress of a piece of the contact line shall be calculated with the following formulae:

$$p_{\mathrm{H}} = \sqrt{\frac{\mathrm{d}F \cdot E_{\mathrm{red}}}{2 \cdot \pi \cdot \mathrm{d}l \cdot \rho_{\mathrm{red}}}} \tag{B.1}$$

$$\rho_{\mathrm{red}} = \frac{\rho_1 \cdot \rho_2}{\rho_1 + \rho_2} \tag{B.2}$$

where

$\mathrm{d}F$ is the force transmitted by the piece of the contact line;

E_{red} is the equivalent E-module;

$\mathrm{d}l$ is the length of the piece of the contact line;

ρ_{red} is the equivalent radius of curvature.

It is assumed that the Hertzian stress is constant along the contact line. Otherwise, strong wear would appear at pieces of the contact line with higher stress and lead to a relief. With this assumption, of a constant Hertzian stress along the contact line, it is possible to resolve the relationship stated above with respect to the force vector, $\mathrm{d}\vec{F}$. The force vector, $\mathrm{d}\vec{F}$, shall be calculated according to Formula (B.3).

$$\mathrm{d}\vec{F} = p_{\mathrm{H}}^2 \cdot \frac{2\pi}{E_{\mathrm{red}}} \cdot \rho_{\mathrm{red}} \cdot \mathrm{d}l \cdot \vec{n} \tag{B.3}$$

$\mathrm{d}\vec{F}$ is the force vector normal to the flanks of the worm wheel and the worm, or expressed in other words normal to the tangential plane mentioned earlier. $\vec{n}$ is the normal vector, that is normal to the two tooth flanks as well as to the tangential plane. Viewing a parallel section (offset plane see ISO 1122-2) leading through the contact point B as shown in Figure B.3, it is possible to represent the apparent torque at the worm wheel, T_2:

$$T_2 = 10^{-3} \cdot \int_l \left(\mathrm{d}\vec{F} \times \vec{r}\right) \cdot \vec{e}_{\mathrm{x}} \cdot \mathrm{d}l \tag{B.4}$$

where $\vec{e}_x$ is an unit vector pointing in direction of the x-axis.

In this case $\vec{r}$ is the radius from the axis of the worm wheel to the contact point B.

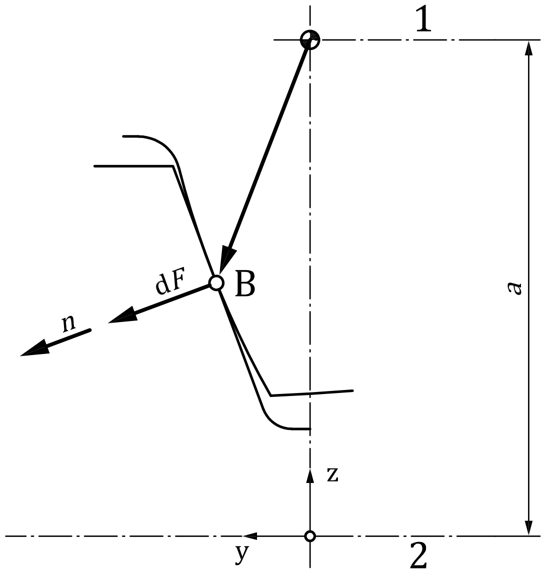

Key

1 axis of worm wheel

2 axis of worm

Figure B.3 — Parallel section through the worm gear set

NOTE Only projection of $\vec{n}$ and $\vec{dF}$ are represented in Figure B.3.

Substituting the force vector to the infinitesimal piece of the contact line with the length of dl calculated in Formula (B.3):

$$T_2 = p_{\mathrm{H}}^2 \cdot \frac{2 \cdot 10^{-3} \cdot \pi}{E_{\mathrm{red}}} \int_l \left(\rho_{\mathrm{red}} \cdot \vec{n} \times \vec{r} \right) \cdot \vec{e}_{\mathrm{x}} \cdot \mathrm{d}l \qquad \text{(B.5)}$$

In this case the integration takes place over the length of all contact lines that are in mesh at the same time. Often there are three teeth in engagement and so the integration has to take place to account for all three contact lines. With the formula of the torque T_2 it is possible to determine the Hertzian stress. For the Hertzian stress, p_{H}:

$$p_{\mathrm{H}} = \frac{4}{\pi} \cdot \sqrt{\frac{T_2 \cdot E_{\mathrm{red}} \cdot 10^3}{a^3} \cdot \left[\frac{\pi}{32} \cdot a^3 \cdot \frac{1}{\int_l \left(\rho_{\mathrm{red}} \cdot \vec{n} \times \vec{r} \right) \cdot \vec{e}_x \cdot \mathrm{d}l} \right]} \qquad \text{(B.6)}$$

The part of Formula (B.6) that is in square brackets consists only of geometrical values. The integral can only be solved by computer programs. This calculation sums up the values to be integrated in dependence of each piece of the contact lines. The value that is in square brackets is named p^*. When p^* is known, it is now possible to calculate the Hertzian stress, p_{H}, from the torque, the equivalent Modulus of elasticity and the centre distance. This Hertzian stress is for a certain position between worm and worm wheel and the contact lines that are in engagement at the same time. When turning worm and worm wheel a little bit further, the contact lines are moving, and those new contact lines lead to a new Hertzian stress, p_{H}. For further calculations the mean value of the Hertzian stress of all investigated positions of the worm may be used. Thus Formula (B.6) for the calculation of the mean Hertzian stress, p_{Hm}, may be restated:

$$p_{Hm} = \frac{4}{\pi} \cdot \sqrt{\frac{T_2 \cdot E_{red} \cdot 10^3}{a^3} \cdot p_m^*} \tag{B.7}$$

with:

$$p_m^* = \frac{\pi}{32} \cdot \frac{a^3}{\int\limits_l \left(\rho_{red} \cdot \vec{n} \times \vec{r}\right) \cdot \vec{e}_x \cdot \mathrm{d}l} \tag{B.8}$$

where p_m^* is the mean value of the geometrical value, p^*, explained before.

Experimental investigations concerning wear and pitting have shown that this mean Hertzian stress, p_{Hm}, has a strong influence. For the calculation of the Hertzian stresses at the worm wheel, the acting torque T_2, the equivalent modulus of elasticity, E_{red}, and the centre distance, a, are known. The value of p_m^* can be calculated by using Formula (B.8).

Similar to what is shown here for the Hertzian stress, the mean lubricant film thickness, $h_{min\,m}$, and the mean sliding path, s_{gm}, can be calculated.

The usual parameters gained in this manner for the Hertzian stress, minimum lubricant film thickness and sliding path are non-dimensional. They have the advantage that they are only dependant on the gearing geometry. Therefore if these parameters are known for a certain gearing, the Hertzian contact stress, the lubricant film thickness and the sliding path can be easily determined for every possible loading, rotational speed and lubricant, corresponding to that gearing.

Annex C
(normative)

Lubricant film thickness according to the Elasto Hydrodynamic Lubrication (EHL) theory

C.1 Principle of calculation

In accordance with Dowson and Higginson[19] and the Elasto Hydrodynamic Lubrication (EHL) theory, the minimum lubricant film thickness, h_{min}, between the flanks along each piece of the contact line dl (See Figure B.1 as localized value for one contact point) shall be calculated as follows:

$$h_{min} = 1{,}6 \cdot \alpha^{0{,}6} \cdot \eta_{0M}^{0{,}7} \cdot E_{red}^{0{,}03} \cdot \rho_{red}^{0{,}43} \cdot (V_{SUMn}/2)^{0{,}7} \Big/ (\mathrm{d}F/\mathrm{d}l)^{0{,}13} \quad \text{(C.1)}$$

where

h_{min} is in µm;

E_{red} is in N/m^2;

ρ_{red} is in m;

$\mathrm{d}F/\mathrm{d}l$ is in N/m;

V_{SUMn} is in m/s, see ISO/TR 10828:2015, 11.5.

A determinant influence factor is the dynamic viscosity, η_{OM}, of the lubricant at ambient pressure and bulk temperature of the worm wheel. Due to temperatures of the worm wheel in large excess of the oil, the oil viscosity shall be considered at the wheel bulk temperature.

The value, $h_{min\,m}$, is calculated on the basis of local values for h_{min}. $h_{min\,m}$ is the mean minimum lubricant film thickness over the entire meshing zone.

For A, I, N, K and C profiles, a zone exists around the centre of the face width of the worm wheel where the projection of the sum of the two velocities along the normal of the piece of the contact line, V_{SUMn}, becomes zero and the conditions of the EHL theory[32], are no longer fulfilled. So a mean value should not be seen as a physical determinant. However, based on the evaluation of test results, the integral usage of the mean value, $h_{min\,m}$, is a relevant parameter.

C.2 Guideline to calculate *h**

For h^*, see 6.4.3.

In the following, units are according to Table 1.

$$h_{\min m} = \frac{1}{\sum_{St} \cdot \sum_{Bl} \mathrm{d}l} \cdot \sum_{St} \cdot \sum_{Bl} \left(h_{\min} \cdot \mathrm{d}l \right) \tag{C.2}$$

From which h^* can be determined:

$$h^* = \frac{(1\,000)^{-0{,}5}}{\sum_{St} \cdot \sum_{Bl} \mathrm{d}l} \cdot \sum_{St} \cdot \sum_{Bl} \left(h_{\min} \cdot \mathrm{d}l \right) \cdot \frac{T_2^{0{,}13}}{21 \cdot c_\alpha^{0{,}6} \cdot \eta_{0\mathrm{M}}^{0{,}7} \cdot n_1^{0{,}7} \cdot a^{1{,}39} \cdot E_{\mathrm{red}}^{0{,}03}} \tag{C.3}$$

After simplification:

$$h^* = \frac{(1\,000)^{-0{,}5}}{\sum_{St} \cdot \sum_{Bl} \mathrm{d}l} \cdot \sum_{St} \cdot \sum_{Bl} \left(1{,}6 \cdot \rho_{\mathrm{red}}^{0{,}43} \cdot \frac{(v_{\Sigma n}/2)^{0{,}7}}{(\mathrm{d}F/\mathrm{d}l)^{0{,}13}} \cdot \mathrm{d}l \right) \cdot \frac{T_2^{0{,}13}}{21 \cdot n_1^{0{,}7} \cdot a^{1{,}39}} \tag{C.4}$$

but from Formula (C.3):

$$\frac{\mathrm{d}F}{\mathrm{d}l} = \frac{2 \cdot \pi}{E_{\mathrm{red}}} \cdot p_H^2 \cdot \rho_{\mathrm{red}} \tag{C.5}$$

but:

$$p_{\mathrm{H}} = \sqrt{T_2 \cdot \frac{E_{\mathrm{red}}}{2 \cdot 10^{-3} \cdot \pi} \cdot \frac{1}{\int\limits_l \left(\rho_{\mathrm{red}} \cdot \vec{n} \times \vec{r} \right) \cdot \vec{e}_x \, \mathrm{d}l}} \tag{C.6}$$

so: (1 000 appears)

$$\frac{\mathrm{d}F}{\mathrm{d}l} = T_2 \cdot \frac{1\,000}{\int\limits_l \left(\rho_{\mathrm{red}} \cdot \vec{n} \times \vec{r} \right) \cdot \vec{e}_x \, \mathrm{d}l} \cdot \rho_{\mathrm{red}} \tag{C.7}$$

$$h^* = \frac{(1\,000)^{-0{,}63}}{\sum_{St} \cdot \sum_{Bl} \mathrm{d}l} \cdot \sum_{St} \cdot \sum_{Bl} \left(1{,}6 \cdot \rho_{\mathrm{red}}^{0.3} \cdot \left(\frac{v_{\Sigma n}}{2 \cdot n_1} \right)^{0{,}7} \cdot \left(\int\limits_l \left(\rho_{\mathrm{red}} \cdot \vec{n} \times \vec{r} \right) \cdot \vec{e}_x \, \mathrm{d}l \right)^{0{,}13} \cdot \mathrm{d}l \right) \cdot \frac{1}{21 \cdot a^{1{,}39}} \tag{C.8}$$

Annex D
(normative)

Wear path definition

The wear path, s_W, covered during life shall be calculated from the number of stress cycles of the wheel N_L, and the sliding path of the worm flank within the Hertzian contact on the wheel flank.

$$s_{Wm} = s_{gm} \cdot N_L \quad \text{(D.1)}$$

Figure B.2 shows the contact line that is normal to the flanks of the worm and the worm wheel.

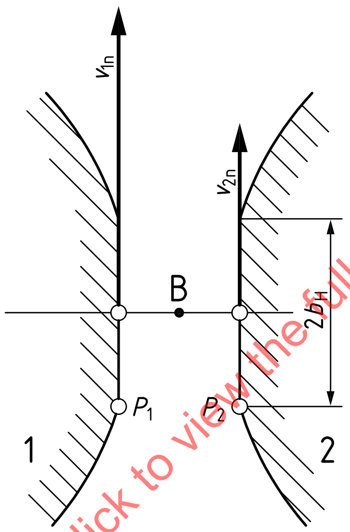

Key

1 the worm flank

2 the worm wheel flank

Figure D.1 — Contact point B of the flanks of the worm and the worm wheel

Unlike Figure B.2, the flanks are shown flattened because of the Hertzian stress in Figure D.1. The width of the flattening amount is $2 \cdot b_H$. Also the actual speeds of the two flanks $\vec{v}_{1n}$ and $\vec{v}_{2n}$ can be seen.

First it should be determined on which local sliding path, s_{gB}, a point, P_2, that belongs to the flank of the worm wheel in the plane of the flattening, moves relatively to the flank of the worm. A stationary movement of the two equivalent flanks relative to the contact lines is required. In reality, of course, the movements are absolutely non-stationary because the position of the contact lines and the position of the curvatures of the both equivalent cylinders change continuously. With this implied stationary condition the flattening at the worm and the worm wheel is timewise constant. A point of the worm wheel, P_2, has the speed $\vec{v}_{2n}$ while moving in the flattening plane. The time of contact shall be:

$$t_{contact} = 2 \cdot \frac{b_H}{\vec{v}_{2n}} \quad \text{(D.2)}$$

Normally only the worm wheel of a worm gear set shows wear, as the worm consists of hardened steel and the worm wheel of bronze. Therefore most important for the wear of the worm wheel is the sliding path of the point, P_2, of the worm wheel in relation to a point, P_1, of the flank of the worm. The affiliated local sliding path, s_{gB}, results from the sliding speed, $\vec{v}_{gB}$, between the two points, P_1 and P_2, and the time of contact, $t_{contact}$. Then for the local sliding path:

$$s_{gB} = \left|\vec{v}_{gB}\right| \cdot t_{contact} \tag{D.3}$$

The sliding speed, $\vec{v}_{gB}$, is the difference between the speeds, $\vec{v}_1$ and $\vec{v}_2$, projected in the common tangent plane of contact. With this the local sliding path shall be calculated with:

$$s_{gB} = \left|\vec{v}_1 - \vec{v}_2\right| \cdot t_{contact} \tag{D.4}$$

Together with Formula (D.2) follows for the local sliding path:

$$s_{gB} = \frac{\left|\vec{v}_{gB}\right|}{\vec{v}_{2n}} \cdot 2 \cdot b_H \tag{D.5}$$

For a worm gear set, the sliding speed, $\vec{v}_{gB}$, shall be built by the following formula because the flanks of the worm and the worm wheel is not only moving normal to the contact line but also in opposite directions on the contact line:

$$\vec{v}_{gB} = \vec{v}_1 - \vec{v}_2 \tag{D.6}$$

The vectors, $\vec{v}_1$ and $\vec{v}_2$, are the speeds of the flanks of the worm and the worm wheel in the tangential plane between the two flanks for a certain contact point.

The local sliding paths are calculated for all infinitesimal neighbouring contact points. Then the mean value of all sliding paths can be calculated. This mean value is named mean sliding path, s_{gm}.

$$s_{gm} = s^* \cdot \sigma_{Hm} \cdot \frac{a}{E_{red}} \tag{D.7}$$

where

σ_{Hm} is the mean Hertzian stress;

a is the centre distance;

E_{red} is the equivalent modulus of elasticity;

s^* is the parameter for the mean sliding path.

s^*, as well as p_m^*, is a pure geometrical value that can be calculated in a similar way with computer programs. In general, it is sufficient to calculate s^* with approximation formulae that can be found in this document.

The local sliding path appears each time when a tooth comes in contact again. The wear path is increased with the number of stress cycles as well as the number of the revolutions of the worm wheel.

Many experimental investigations have shown that the wear path, s_W, is an important value for the behaviour of the wear of a worm gear set.

As an example, the procedure for the calculation of the mean sliding path, s_{gm}, is shown here; it is the integral mean value of the total local sliding paths, s_{gB}, over the total meshing zone. See Figure D.2.

For the mean sliding path, s_{gm}, the following mean values are calculated:

— the mean local sliding path, s_{gB}, in each contact line section (dl) between two contact points;

— mean value over the contact lines (N_{BL}) which are simultaneously present at the worm position;

— mean value between the calculated position (N_{St}) of a load cycle.

Thus the mean value for the contact shall be:

$$s^* = \frac{1}{\sum_{N_{St}} \cdot \sum_{N_{BL}} \mathrm{d}l} \cdot \sum_{N_{St}} \cdot \sum_{N_{BL}} \left(s_{gB} \cdot \mathrm{d}l\right) \cdot \frac{E_{red}}{a} \cdot \frac{1}{\sigma_{Hm}} \tag{D.8}$$

where

N_{St} is the number of calculated positions;

N_{BL} is the number of contact lines for one calculated position. Figure B.1 shows a contact line on the worm wheel.

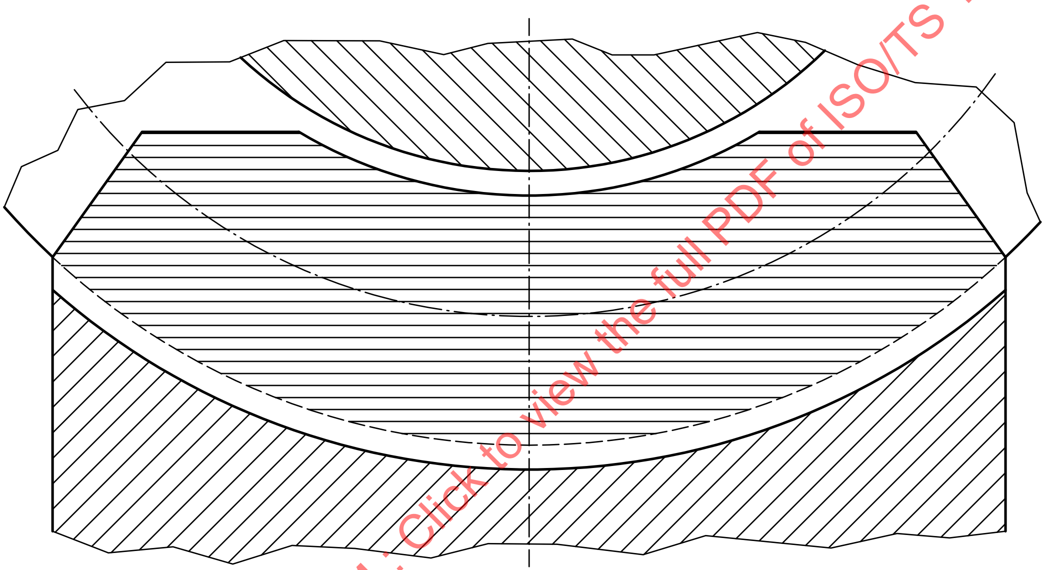

Figure D.2 — Example of contact line calculation (projection in wheel plane)

Annex E
(informative)

Notes on calculation wear

The calculation procedure described here is based on tests run with bronze wheels and oil, both of which are from a single batch. Experience to date shows that considerable influences can be associated with material and oil. Test and operational experience show that wear values undergo a very large scattering and classification of unknown lubricant, even with known base oils, is only possible within limits. With the wear relationship investigation stated here, only the investigated pairings are, in principle, calculable.

Furthermore, the following restrictions can be observed:

— The calculation is only valid for constant power and gears that have been run-in. Wear peaks due to overloading or impermissible oil temperatures are **not** considered.

— The calculation is only valid for case hardened and ground worms and $Ra_1 \leq 0{,}5$ µm; larger roughness can cause considerable increases in the wear, especially during the run-in.

Annex F
(informative)

Notes on tooth root strength

The calculations only apply to the root strength of the wheels' teeth when coupled with worms made of 16MnCr5 steel case hardened. During experiments concerning endurance limit and the region of time strength, the wheels' teeth tend to break in the case of gear pairs with bronze wheels; in the case of wheels made of grey cast and nodular cast materials, the worm threads break.

The endurance strengths for the plastically deforming materials (CuSn — bronzes) are already partially in the plastic range. If small plastic deformations are permissible, these values can be calculated. Otherwise reduced strength values should be used. Average values for perfect structures have been taken as the basis for the yield point. The time strength of these wheels can be understood as a sort of damage line which runs in the plastic range and is limited by the definition of a permissible accuracy grade deterioration (plastic deformation) of the worm wheel.

For the more brittle and harder aluminium bronze alloy, the difference between the plastic and elastic deformations is smaller.

For grey cast iron and nodular iron the endurance and time strength values lie in the elastic region.

When determining the shear stress the reduction of the tooth root chord due to abrasive wear can be taken into account, since this weakens the wheel tooth. The wheel tooth can also be weakened by a high pitting depth. This however can not be taken into account due to inconclusive calculations.

Annex G
(informative)

Adaptation of formulae for the reference gear with results from testing

Certain formulae of this document can be refined by experience from carefully controlled worm gear drive tests. The procedure is introduced in Clause 4 with the keyword 'relative calculating'. This annex explains these considerations.

The formulae in this document are based on a variety of experiments, mostly using the standard ISO/TS 14521 test gear with the centre distance a_T = 100 mm. The centre distance a of the gear to be calculated usually differs from a_T. The results found by experiments with the standard gear need to be transferred to the conditions of the gear to be calculated. This document provides the necessary relationships. As an example, Formulae (38) and (39) for the calculation of the idle running power loss, P_{V0}, are used:

$$P_{V0} = 0{,}89 \cdot 10^{-2} \cdot \frac{a}{a_T} \cdot n^{4/3} \tag{G.1}$$

$$P_{V0} = 0{,}89 \cdot 10^{-2} \cdot \frac{a}{100} \cdot n^{4/3} \tag{G.2}$$

The accuracy of this formula decreases as more as a differs from a_T. Supposed experiments with a centre distance closer to the centre distance a of the gear to be calculated are available. Using this experiment as base for the Formula (G.1) will improve the accuracy of calculation. Figure G.1 shows an example: ISO/TS 14521 test gear with a_T = 100 mm, a gear to be calculated with a centre difference a = 400 mm and a new test gear with a_{T1} = 500 mm.

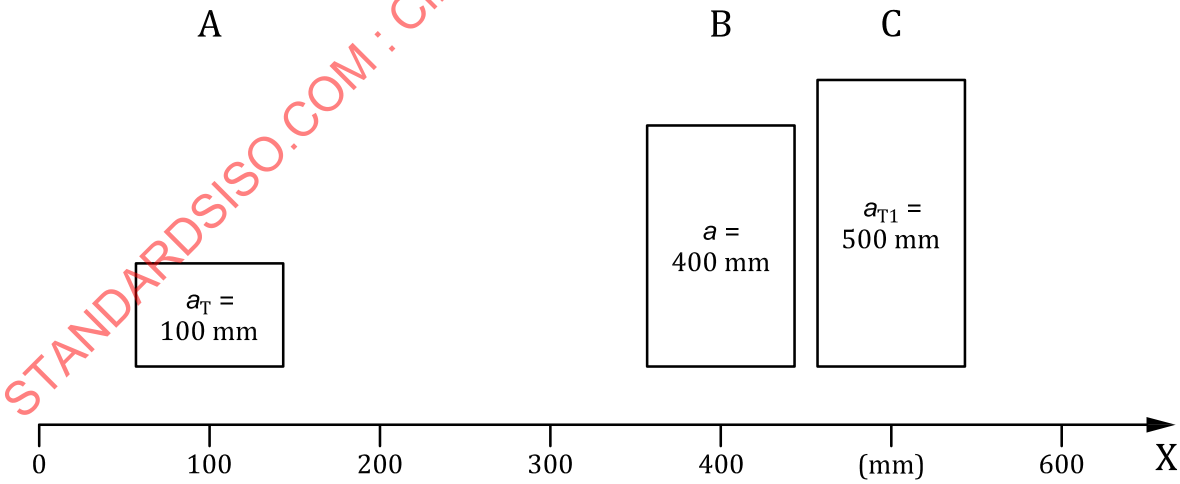

Key

X centre distance a

A ISO/TS 14521 test gear

B gear to be calculated

C new test gear

Figure G.1 — Centre distances of two test gears and a gear to be calculated

Analogue to Formula (G.1), measurements of idle running power losses at the gear with the centre distance $a_{T,1}$ lead to the following formula.

$$P_{V0,1} = K_1 \cdot \frac{a}{a_{T1}} \cdot n^{4/3} \tag{G.3}$$

For experiments on the new test gear $a_{T,1} = a = 500$ mm Formula (G.3) resolves to

$$P_{V0,1} = K_1 \cdot \frac{500}{500} \cdot n^{4/3} \tag{G.4}$$

With measurement results, $P_{V0,1\ \text{measured}}$, for the idle running power loss, the factor, K_1, can be calculated by transforming Formula (G.4) into

$$K_1 = \frac{P_{V0,1\text{measured}}}{n^{4/3}} \tag{G.5}$$

Now two functions exist for the calculation of the power loss. In the example, there is one function for a test gear with the centre distance $a_T = 100$ mm and a second one for a gear with the centre distance $a_{T,1} = 500$ mm. Certainly both functions have exact results for their respective test centre distances about 100 mm or 500 mm.

The more the centre distance of the gear to be calculated differs from the centre distances of the test gears, the less accurate the formulae get. This results in a deviation ΔP_{V0} between the real idle running power loss and the value obtained by the formulae. Figure G.2 shows that deviation ΔP_{V0} for a P_{V0} calculated by the ISO test gear with $a_T = 100$ mm (curve T) and for a P_{V0} calculated for the new test gear with $a_{T1} = 500$ mm (curve T1).

In this example it is assumed that the deviation ΔP_{V0} decreases with 5 % when the centre distance changes about 100 mm starting from the centre distance the test gear. The difference of the centre distances between the new test gear and the gear to be calculated is much smaller (100 mm) than the difference to the centre distances of the ISO test gear (300 mm). Therefore the deviation of the idle running power loss for the new test gear $\Delta P_{V0}(a_{T1} = 500)$ is less than $\Delta P_{V0}(a_T = 100)$ for the ISO test gear.

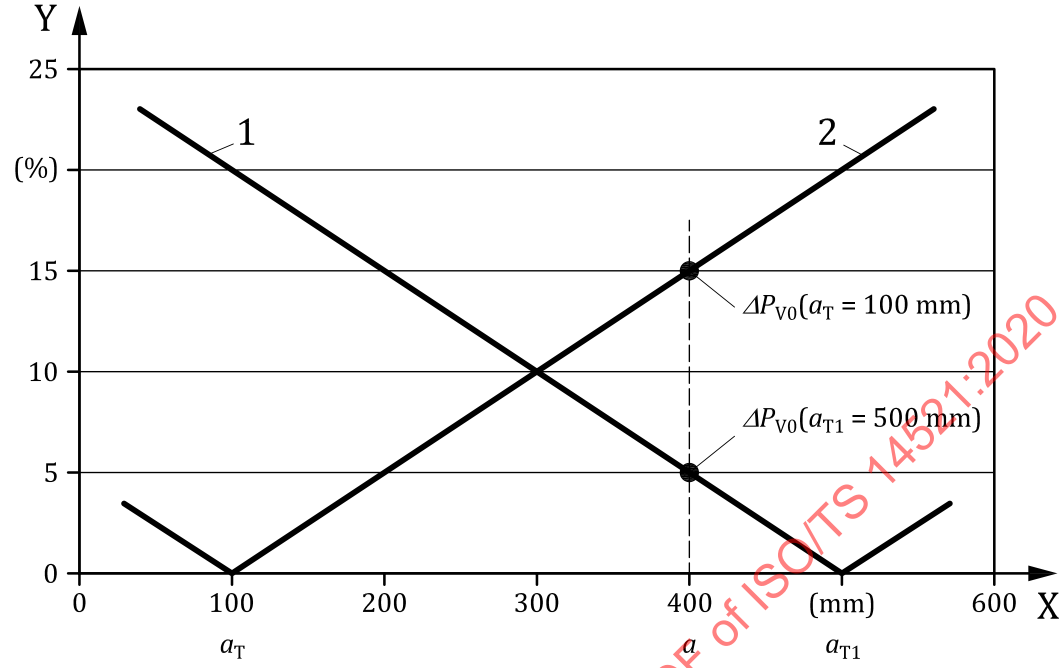

Key

X centre distance, a

Y deviation, ΔP_{V0}

1 curve T1

2 curve T2

Figure G.2 — Deviations ΔP_{V0} for two test gears

This example shows how the formulae of this document can easily adopted to experiments with operating conditions closer to the gear to be calculated than the operating conditions of the ISO standard test gear, improving the quality of the calculated results.

Annex H
(informative)

Life time estimation for worm gears with a high risk of pitting damage

In this annex a life time estimation for worm gears with a high risk of pitting damage on the basis of the wear load calculation is shown. The life time of such a worm gear drive can be divided into three characteristic stages:

— Stage I: Stage of beginning of pitting, number of load cycles N_{LI}

— Stage II: Pitting growth stage, number of load cycles N_{LII}

— Stage III: Wear stage, number of load cycles N_{LIII}

The numbers of load cycles in the stages I to III can be combined according to Formula (H.1) to a total number of load cycles N_L:

$$N_L = N_{LI} + N_{LII} + N_{LIII} \tag{H.1}$$

Stage I covers the time up to the first pitting. The first pitting is defined by the pitting area A_{P10} = 2 %. The number of load cycles N_{LI} in stage I, which depends on the specific operating conditions, can be calculated according to Formula (H.2) in dependence of σ_{Hm} and v_{gm}:

$$N_{LI} = 10^6 \cdot \left(1 + 0{,}860 \cdot \ln\left(3 \cdot \frac{v_g}{v_{ref}}\right)\right) \cdot \exp\left[28{,}078 - 4{,}666 \cdot \ln\left(520 \cdot \frac{\sigma_{Hm}}{\sigma_{Hlim}}\right)\right] \tag{H.2}$$

with v_{ref} = 3 m/s, v_{gm} according to Formula (9), σ_{Hlim} from Table 9 and σ_{Hm} according Formula (19)

Stage II, characterized by pitting growth, follows directly the stage of beginning of pitting (stage I) and stops when the maximum pitting area $A_{P10,max}$ is reached. For a given (allowable) pitting area $A_{P10,max}$ (2 % to 60 %) the number of load cycles N_{LII} can be calculated according to Formula (H.3) ($A_{P10,max}$ is in %):

$$N_{LII} = \frac{\left(A_{p10,max} - 2\right).10^6}{16{,}212 . \dfrac{(\sigma_{Hm} - 180)}{\sigma_{Hlim}} . \exp\left[1{,}541 \dfrac{\sigma_{Hm}}{\sigma_{Hlim}} - 0{,}581 . \dfrac{v_g}{v_{ref}}\right]} \tag{H.3}$$

The following plausibility check should be made. It must be:

$$N_{LI} + N_{LII} \leq N_{L(I+II)} \tag{H.4}$$

with:

$$N_{L(I+II)} = 3 \cdot 10^6 \cdot \frac{v_g}{v_{ref}} \cdot \exp\left[24{,}924 - 4{,}047 \cdot \ln\left(520 \cdot \frac{\sigma_{Hm}}{\sigma_{Hlim}}\right)\right] \tag{H.5}$$

The reduction of the pitting area in stage III is based on the wear behaviour in this stage. The number of load cycles in stage III, N_{LIII}, can be determined with Formula (H.1). The number of load cycles, N_{LIII}, is only reached, if there is a sufficient wear safety. The wear safety is determined according to Reference [24]. It has to be regarded that, instead of the wear intensity, J_W, respectively the flank loss,

δ_{Wn}, the wear intensity, J_{WP}, respectively the flank loss, δ_{WPn}, according to Formula (H.6) respectively (H.7) have to be used.

$$J_{WP} = W_{ML} \cdot W_{NS} \cdot \left[J_{0I} \cdot \frac{N_{LI}}{N_L} + 0{,}5 \cdot (J_{0I} + J_{0III}) \cdot \frac{N_{LII}}{N_L} + J_{0III} \cdot \frac{N_{LIII}}{N_L} \right] \tag{H.6}$$

The wear intensity, J_{0I}, can be calculated by using Formulae (69) to (79), the wear intensity, J_{0III}, by using Formula (H.7).

$$J_{0III} = W_P \cdot J_{0I} \tag{H.7}$$

The damage factor, W_P, can be calculated by using (H.8).

$$W_P = 25 \cdot K_W^{0{,}75} \tag{H.8}$$

This calculation procedure is based on tests, which cover the following boundary conditions:

— Working mode:	constant with running-in
— Mean contact stress σ_{Hm}:	330 N/mm² to 620 N/mm²
— Mean sliding velocity v_{gm}:	1 m/s to 7,5 m/s
— Centre distance a:	65 mm to 160 mm
— Nominal ratio i_N:	10 to 20
— Arithmetic mean roughness Ra:	0,4 µm to 0,5 µm
— Material combination:	16MnCr5E/CuSn12Ni2-C-GZ
— Lubrication:	Polyglycol ISO VG 220 at θ_{oil} = 80 °C

For worm gear drives, which are in between these boundary conditions, this calculation procedure shows good results. For other boundary conditions the calculation should be verified by tests if possible.

Annex I
(informative)

Examples

I.1 Example — Calculation of the efficiency and the safety factors for a standard reference gear (flank form I) with given loading

Given:

centre distance	a = 100 mm
gear ratio	u = 41 : 2
normal pressure angle	$\alpha_0(=\alpha_n)$ = 20°
axial module of worm	m_{x1} = 4 mm
reference worm diameter	d_{m1} = 36 mm
reference worm wheel diameter	d_{m2} = 164 mm
worm wheel root diameter	d_{f2} = 154,4 mm
worm wheel face width	$b_{2R} = b_{2H}$ = 30 mm
rim thickness of worm wheel	s_K = 8 mm
worm bearing spacing (symmetrical)	l_1 = 150 mm
output power	P_2 = 4,5 W
ambient temperature	θ_0 = 20 °C
input rotational speed	n_1 = 1 500 min^{-1}
required life expectancy with continuous operation	L_h = 25 000 h;
material combinations: worm, 16 MnCr5, case hardened and ground, wheel	GZ — CuSn12Ni2;
arithmetic mean roughness of the worm flanks	Ra_1 = 0,5 µm
lubrication with polyglycol,	ν_{40} = 220 mm^2/s,
	ν_{100} = 37 mm^2/s
density of lubricant	ρ_{oil15} = 1,02 kg/dm^3
splash lubrication (wheel immersed), gear with fan.	
Sought: efficiency and safety factors with an application factor	K_A = 1,0

Calculated (general quantities):

addendum modification factor see ISO/TR 10828	$x_2 = 0$
output torque	$T_2 = 60/(2\cdot\pi) \cdot P_2 \cdot u/n_1 = 587{,}28$ Nm
peripheral force see ISO/TR 10828	$F_{tm2} = 7\,161{,}97$ N
lead angle according to Formula (5)	$\gamma_{m1} = 12{,}53\,°$
diameter quotient	$q_1 = 9$
sliding velocity according to Formula (9)	$v_g = 2{,}896$ m/s
standard worm wheel face width according to Formula (10)	$b_{2H,std} = 30{,}83$ mm
worm wheel face width factor for p_m^* according to Formula (13)	$f_p = 1{,}002\,7$
parameter for the mean Hertzian stress according to Formula (11)	$h^* = 0{,}949\,6$
worm wheel face width factor for p_m^* according to Formula (16)	$f_h = 0{,}996\,07$
parameter for the mean lubricant film thickness according to Formula (14)	$h^* = 0{,}068\,91$
parameter for the mean sliding path according to Formula (17)	$s^* = 30{,}285$
mean contact stress according to Formula (19)	$\sigma_{Hm} = 369{,}02$ N/mm^2

Calculated (efficiency):

base coefficient of friction according to Formula (54)	$\mu_{OT} = 0{,}024$
mean coefficient of friction according to Formula (48)	$\mu_{zm} = 0{,}023$ with $Y_S = 1$, $Y_G = 1{,}008$, $Y_W = 0{,}95$ and $Y_R = 1$
gear efficiency according to Formula (46)	$\eta_{z1\text{-}2} = 89{,}98$ %
total power loss according to Formula (37)	$P_V = 0{,}805$ W,
with meshing power loss according to Formula (63)	$P_{Vz1\text{-}2} = 0{,}478$ W,
idle running power loss according to Formula (38)	$P_{V0} = 0{,}153$ W,
bearing power loss (adjusted bearings) according to Formula (40)	$P_{VLP} = 0{,}128$ W,
and sealing power loss according to Formula (44)	$P_{VD} = 0{,}046$ W, for two sealing lips
total efficiency according to Formula (35)	$\eta_{ges} = 84{,}8$ %.

Calculated (wear):

oil sump temperature according to Formula (117)	θ_S = 73,2 °C
	for housings with fan
wheel bulk temperature according to Formula (130)	θ_M = 77,2 °C
	with α_L = 24 440 W/(m^{2}K) and A_R = 0,004 9 m^2
lubricant density at wheel bulk temperature according to Formula (26)	ρ_{OilM} = 0,97 kg/dm^3
kinematc viscosity at wheel bulk temperature according to Formula (32)	ν_M = 65,07 mm^2/s
dynamic viscosity at wheel bulk temperature according to Formula (25)	η_{0M} = 0,06 Ns/m^2
lubricant structure factor according to Formula (82)	W_S = 2,63
pressure factor according to Formula (84)	W_H = 1
mean lubricant film thickness according to Formula (21)	$h_{\min m}$ = 0,245 µm
mean sliding path according to Formula (30)	s_{Wm} = 814 361 mm
parameter according to Formula (80)	K_W = 0,643
start factor according to Formula (83) for continual operation	W_{NS} = 1
material-lubricant factor according to Table 7	W_{ML} = 1,75
reference wear intensity according to Formula (74)	J_{0T} = 51,87 · 10^{-11}
wear intensity according to Formula (68)	J_W = 90,76 · 10^{-11}
flank loss according to Formula (67)	δ_{Wn} = 0,739 mm
limiting value for the max. permissible flank loss according to Formula (90)	
(indicated by backlash)	$\delta_{W\lim n}$ = 1,17 mm
wear safety factor according to Formula (65)	S_W = 1,6.

Calculated (pitting):

limiting value for the contact stress according to Formula (93)	σ_{HG} = 442,77 N/mm^2
	with Z_h = 1,
	Z_v = 0,85,
	Z_u = 1,
	Z_s = 1 and
	Z_{oil} = 1
pitting safety factor according to Formula (91)	S_H = 1,2